Materials Advances

ROYAL SOCIETY OF CHEMISTRY

REVIEW

View Article Online
View Journal | View Issue

Cite this: *Mater. Adv.*, 2025, **6**, 7634

Lead-free perovskites for next-generation applications: a comprehensive computational and data-driven review

Syeda Kinza Fatima,[ab] Reem H. Alzard,*[c] Riffat Amna,[d] Mohammed H. Alzard,[ce] Kaibo Zheng[fg] and Mohamed Abdellah *[c]

Lead-free perovskites (LFPs) are an emergent class of materials with great potential as next-generation candidates for energy and optoelectronic applications, offering a sustainable and non-toxic alternative to their lead-based counterparts. Computational studies play a central role in accelerating the discovery, design, and optimization of these materials by enabling predictive insights into electronic, optical, and device-level behavior. This review presents a comprehensive analysis of the computational landscape surrounding lead-free perovskites, combining bibliometric mapping, methodological classification, and thematic exploration across material types and application domains. A total of 200 peer-reviewed articles published between 2013 and 2025 were analyzed, offering a comprehensive picture of how computational tools from density functional theory (DFT) to machine learning (ML), and device-level simulation have shaped LFP research. The review highlights the dominant role of photovoltaic modeling and the growing diversification of lead-free perovskite research into applications such as thermoelectrics, spintronics, photocatalysis, neuromorphic computing, radiation detection, thermal barrier coatings, gas sensing, and ferroelectric systems. Density functional theory remains the foundational tool, supported by increasingly sophisticated approaches such as high-throughput screening and device-level simulation. The novelty of this study lies in its data-driven, cross-scale synthesis that links computational strategies to targeted properties and application outcomes of lead-free perovskites. It outlines strategic initiatives through which theory and simulations have driven the discovery and optimization of high-performance, stable LFPs, while identifying emerging trends and future directions in the evolving role of computational science in materials innovation.

Received 26th June 2025,
Accepted 20th August 2025

DOI: 10.1039/d5ma00681c

rsc.li/materials-advances

1. Introduction

Perovskite materials have become a revolutionary class of semiconductors with outstanding optoelectronic qualities that have spurred the development of photovoltaics, light-emitting devices, and photodetectors.[1,2] Foremost among these are lead-halide perovskites, whose power conversion efficiencies are rising rapidly, and they are also processable at a low cost, placing them at the forefront of the next wave of solar technologies.[3] A major hindrance to the large-scale deployment of the material is the toxicity of lead, a heavy metal with considerable implications for both the environment and human health.[4,5] The volatile nature of the lead-degradation products under operating conditions further compounds long-term stability and regulatory issues.[6,7]

In response to such limitations, the quest for LFP has gathered speed. Unlike cation substitution alone, the synthesis of functional LFP needs a re-evaluation of structural and electronic design strategies. Initial studies have shown that direct substitution for lead tends to lead to diminished performance because of adverse band alignments, decreased defect tolerance, and lower phase stability.[8,9] Such challenges are not unique to perovskites, as similar trap-mediated limitations have also been observed in semiconductor photocathodes, where surface ligands can outcompete productive charge

[a] *Department of Chemistry, Kunsan National University, Gunsan, Jeonbuk 54150, Republic of Korea*
[b] *Department of Environmental Sciences, COMSATS University Islamabad, Abbottabad Campus, 22020 Abbottabad, Pakistan*
[c] *Department of Chemistry, UAE University, P.O. Box 15551, Al-Ain, United Arab Emirates. E-mail: reem.alzard@uaeu.ac.ae, moabdellah@uaeu.ac.ae*
[d] *Department of Civil and Environmental Engineering, Khalifa University of Science and Technology, P.O. Box 127788, Abu Dhabi, United Arab Emirates*
[e] *Institute of Sustainable Building Materials and Engineering Systems, Riga Technical University, Riga, Latvia*
[f] *Division of Chemical Physics and NanoLund, Lund University, P.O. Box 124, 22100 Lund, Sweden*
[g] *Department of Chemistry, Technical University of Denmark, DK-2800, Kongens Lyngby, Denmark*

transfer,[10] and in quantum-dot/metal-oxide systems where photodegradation critically alters charge-transfer dynamics and long-term stability.[11] As a result, the field initially faced the challenge of finding materials that could rival the multifunctional performance of the lead-based analogues.

The addition of computational material science to the discovery process changed the direction of LFP research. The systematic study of the structural, electronic, and thermodynamic characteristics of lead-free perovskites was made possible by the first-principles method known as density functional theory (DFT).[12] For a wide range of compositions, DFT has been widely used to investigate bandgaps, formation energies, stability, and defect tolerance.[8,13] Large-scale exploration of vast chemical spaces has been prompted by the theoretical underpinnings created by such computations, which are followed by pipelines that integrate machine learning algorithms with high-throughput computational screening.[14,15] High-throughput routines automate the calculation of structural and property information for hundreds or thousands of candidate compounds, and machine learning algorithms learn from the datasets to make quick predictions of such descriptors as bandgap, formation energy, and tolerance factors.[16,17] The combined methodology not only reduces the computational expense of large-scale screening but also facilitates tailoring of the perovskite structure for targeted functionalities *via* inverse design and multi-objective optimization. Altogether, the methodologies have been crucial for expanding the scope, enhancing the speed, and improving the accuracy of lead-free perovskite studies.

However, the most extensively researched area continues to be the photovoltaic one, both computationally and experimentally. More notably, however, LFPs are making increasingly significant strides in a broader technology space that encompasses photocatalysis,[18] thermoelectrics,[19] neuromorphic computing,[20] and thermal insulation.[21] The expanding functional domain is directly related to the predictive capability of computational tools.

To understand how computational approaches have reshaped the discovery and application of LFPs, this review conducts a systematic, data-driven analysis of 200 studies published between 2013 and 2025. The primary objectives are to:

- Map the evolution of computational methods used in LFP research.
- Categorize material subclasses and their associated application domains.
- Identify how specific modeling strategies have enabled progress across different technological areas.

Unlike earlier reviews, this work combines bibliometric mapping with thematic and methodological classification, offering a holistic analysis that connects computational techniques to material development and functional deployment. This integrative perspective provides a new framework for understanding the role of simulation in advancing sustainable perovskite technologies. To demonstrate this in greater detail, the review is concluded with an in-depth analysis of photovoltaic applications, which represent the most methodologically mature and computationally optimized area within LFP research.

2. Background

2.1. Structural diversity and design landscape of lead-free perovskites

The development of LFPs addresses a pivotal challenge in the advancement of optoelectronic and energy materials. The goal is to maintain the excellent performance attributes of lead perovskites while addressing the related environmental and toxicity issues.[10,22] Even though photovoltaics still dominate research, LFPs are becoming more popular in several new applications, including scintillation,[23] thermoelectrics,[24] photocatalysis,[25] and neuromorphic computing.[26] It is enabled by the intrinsic structural versatility of the perovskite architecture as well as the chemical diversity of its components.[27]

At the core of perovskite chemistry is the ABX_3 structure with A as a large monovalent or divalent cation like Cs^+, MA^+, or FA^+, B as a small metal cation, and X as usually a halide, an oxide, or a chalcogenide. The replacement of Pb^{2+} at the B-site is not trivial. Isovalent replacement with Sn^{2+} or Ge^{2+} preserves the ABX_3 motif but tends to result in quick oxidation and instability.[28] Heterovalent strategies involve monovalent–trivalent cation pairs, such as Ag^+ with Bi^{3+} or Sb^{3+}.[29] These combinations give rise to double perovskites with the formula $A_2B'B''X_6$ and to vacancy-ordered structures such as A_2BX_6 and $A_3B_2X_9$.[25,30,31] Various of these materials offer improved chemical durability but exhibit distinct band structures and transport properties.

Structural dimensionality further expands the design space. Fully three-dimensional frameworks support efficient charge transport but are often sensitive to moisture and oxygen. Low-dimensional materials, including two-dimensional layered perovskites, one-dimensional chains, and zero-dimensional cluster-based frameworks, offer better environmental stability and tunable optical behavior, although often with reduced carrier mobility.[32,33] Structural diversity within LFPs enables precise tailoring for targeted applications, including solar energy conversion, light emission, and thermal management.[27]

Given their broad diversity, LFPs can be classified using multiple overlapping criteria as shown in Fig. 1. These include anion chemistry (*e.g.*, halide, oxide, chalcogenide), structural dimensionality (3D to 0D), B-site configuration (single, double, or vacancy-ordered), and bonding character (ionic to covalent). These types are not exclusive. For instance, $Cs_2AgBiBr_6$ is a 3D double perovskite halide. $BaZrS_3$ is a 3D network chalcogenide with ionic as well as covalent bonding characteristics.[34]

The optimal configuration of LFP involves meticulous consideration of critical parameters such as bandgap, thermal stability, ambient stability, low binding energy of the excitation, strong defect tolerance, and good carrier mobility.[35] The enormously vast multidimensional configuration space is not

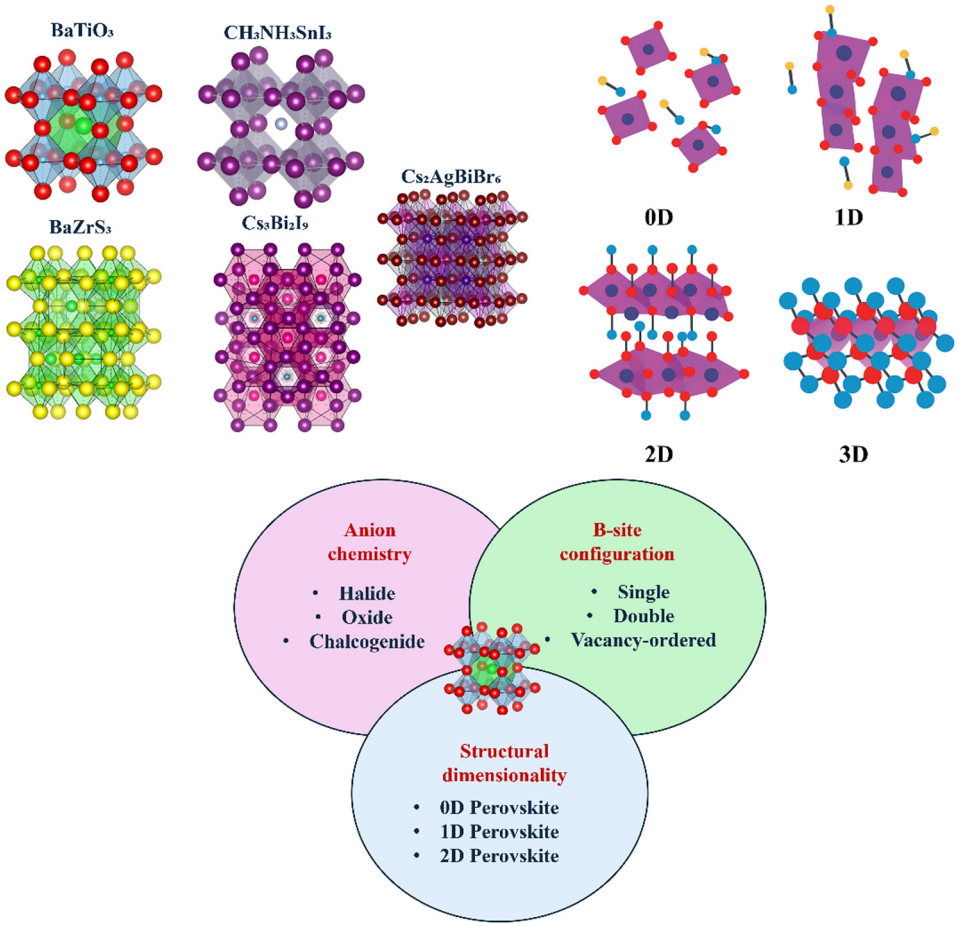

Fig. 1 Classification of lead-free perovskites based on anion chemistry, B-site configuration, and structural dimensionality, with representative crystal structures illustrating the diversity of LFP subclasses.

efficiently searchable by experiment. Computational means such as the use of machine learning algorithms and high-throughput screening are now essential in such cases. They facilitate the prediction of stability, electronic properties, and defects in a quick and efficient manner, thereby speeding up the identification of candidate LFPs in various fields.[14,15]

2.2. Computational approaches for lead-free perovskite design

The search for LFPs is one of the most formidable design tasks in contemporary materials science. Compared to their lead-halide counterparts, there are no mature experimental databases, established stability protocols, or standardized synthesis procedures[33,36] for LFPs. Scientists must optimize electronic, optical, and structural performance across a vast and chemically diverse compositional space, much of which remains unexplored.[13] Computational tools have emerged as indispensable means of exploring uncertainty, advancing discovery, and directing experimental validation, as indicated in Fig. 2. These techniques compensate for the lack of empirical evidence while enabling atomistic understanding of the structure–property relationships underlying LFP functionality.[15,37]

2.2.1. Early methods and first-principles advances. In the early stages of LFP research, computational analysis primarily relied on empirical screening based on geometric parameters such as the Goldschmidt tolerance factor and the octahedral factor, which offered simple estimations of perovskite formability.[27,38] However, these heuristics performed poorly in low-symmetry or compositionally complex systems. The advent of first-principles methods marked a significant breakthrough. The quantum-mechanical framework of DFT enabled the analysis of formation energies, band structures, phonon properties, and defect energies with improved accuracy.[13,39] This facilitated the prediction of the main factors governing material performance and stability. These methods have been applied to predict the behavior of systems such as $MASnI_3$ and $Cs_2AgBiBr_6$ enabling property tuning before synthesis.[10,40]

2.2.2. High-throughput screening and machine learning. As the field progressed, computational approaches expanded from targeted characterization to large-scale discovery. High-throughput (HT) screening, enabled by automated DFT workflows, allows systematic evaluation of thousands of candidate compositions for properties such as band structure, thermodynamic stability, and optical response.[16,41] Extensive

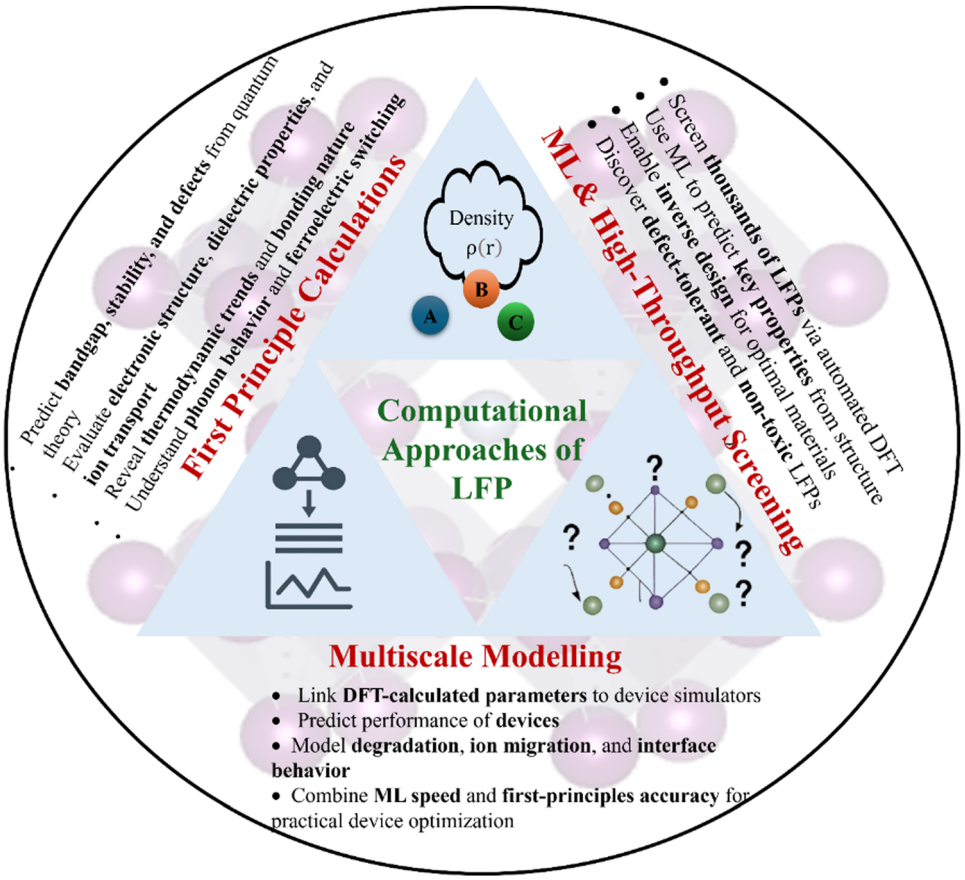

Fig. 2 Schematic overview of computational approaches used in LFP research.

DFT-computed datasets from open-access repositories such as the Materials Project, OQMD, and AFLOW form the foundation of these efforts.

Recent advances couple HT screening with machine learning to accelerate the identification of LFPs, as illustrated in Fig. 3. In such pipelines, chemically and structurally derived descriptors are extracted from existing datasets and used to train predictive models, including gradient boosting methods, support vector regression, and convolutional neural networks. These models, validated against high-fidelity DFT data, enable rapid exploration of vast chemical spaces, supporting inverse design in which new compositions are proposed to meet targeted stability and optoelectronic requirements.[42,43] Predictions are iteratively refined through DFT validation, and, ultimately, experimental synthesis, transforming computational tools from retrospective validation into proactive drivers of discovery. The successful *in silico* prediction and subsequent synthesis of $Cs_2AgBiBr_6$ exemplifies the predictive power of this integrated approach.[44] Remaining challenges include limited availability of high-quality datasets for LFPs, the difficulty of transferring models to unexplored chemistries, and the absence of standardized stability metrics, all of which must be addressed to fully realize the potential of HT–ML discovery frameworks.[45]

2.2.3. Multiscale modeling and modern developments. Modern computational strategies for LFPs increasingly rely on multiscale modeling, which links atomic-level simulations to mesoscale and device-level performance predictions.[46] Multiscale modeling, as shown in Fig. 4 demonstrates how integrated computational approaches expand the application scope of lead-free perovskites. At the atomistic scale, first-principles methods provide key descriptors such as ionic migration barriers, defect energetics, and stability under thermal and environmental stress. These parameters are then integrated into higher-scale simulations, including kinetic Monte Carlo for transport processes, and SCAPS-1D for current–voltage, and efficiency predictions, creating a quantitative bridge from fundamental material properties to device performance metrics.[47,48] As shown in Fig. 5, experimental approaches to LFP have progressed from purely empirical methods to advanced techniques that integrate multiple scales of investigation.

Machine learning further accelerates this process by rapidly screening vast compositional spaces, refining stability descriptors, and enabling inverse design. For example, the proactive searching progress (PSP) workflow combined multiple tree-based ensemble models with Shapley additive explanations to search over 8.2×10^{18} possible lead-free perovskite compositions, down-selecting a small set of promising candidates that were subsequently validated through first-principles calculations and accelerated-aging experiments.[49] This illustrates how interpretable ML can guide high-value simulations, and

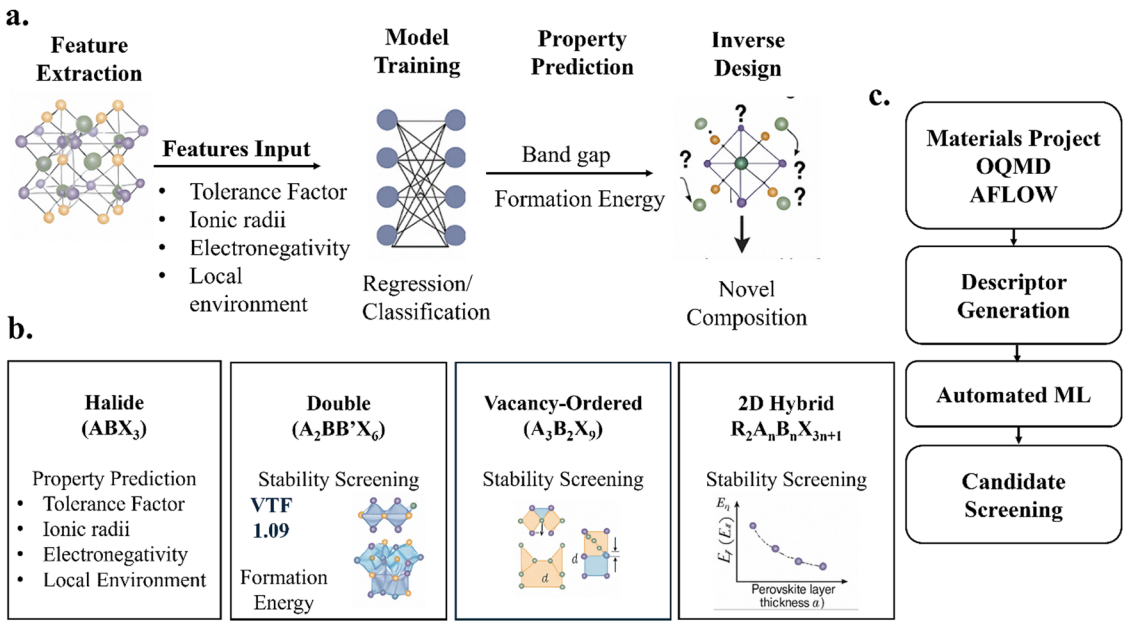

Fig. 3 Machine learning and high-throughput screening approaches for accelerated discovery of lead-free perovskites. (a) Generalized ML workflow, (b) applications of ML to lead-free perovskites and (c) data-driven pipeline linking open databases.

experiments while significantly reducing search time. Table 1 embodies key milestones towards LFP-specific computational methodologies, recording how the area has developed from early empirical screening towards multiscale, and hybrid, and from non-autonomous to increasingly autonomous discovery procedures.[50,51]

2.3. Integrating computational and experimental frameworks

The applicability of computational techniques to real-world devices depends on effective integration with experimental workflows. Hierarchical validation across scales ensures that parameters derived from atomistic and mesoscale simulations align with device-level measurements, while standardized stability indicators normalize results across variations in temperature, humidity, and illumination.[62,63] Closed-loop approaches, where experimental feedback informs model retraining, are particularly valuable for LFPs, given the absence of mature experimental databases and consistent stability protocols.[64–66]

Despite the progress, several gaps remain. Interfacial degradation processes and grain boundary physics are incompletely understood and poorly parameterized. Transferable interatomic potentials for complex lead-free chemistries are scarce.[65] Experimental datasets are often heterogeneous, lacking consistent metadata or measurement protocols, which undermines reproducibility.[45] Furthermore, each method has strengths and limitations. First-principles calculations are unmatched for mechanistic accuracy but are limited to small systems and short timescales.[66] High-throughput DFT extends coverage but still struggles with complex interfaces and finite-temperature effects. Machine learning excels at rapid screening and pattern discovery but depends heavily on the quality and diversity of its training data.[67] Machine learning interatomic potentials can model larger systems, such as grain boundaries and amorphous regions, yet require extensive, high-fidelity training sets to ensure transferability. Mesoscale models are well-suited for studying long-term transport and degradation but cannot capture underlying quantum-level mechanisms without reliable parameterization.[68]

Addressing these limitations will require open, standardized databases that couple structural, processing, and performance metrics, benchmark tasks for cross-scale validation, and uncertainty-aware modeling that identifies when predictions fall outside the model's reliable domain.[45] Bridging these gaps will be essential to ensure that computationally designed LFPs are not only theoretically promising but also manufacturable, scalable, and stable under real-world operating conditions.

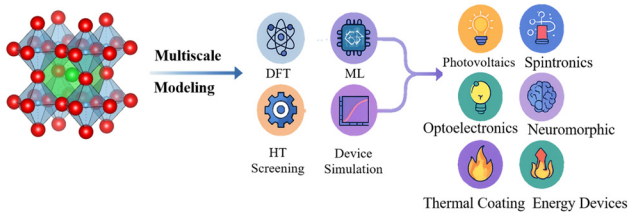

Fig. 4 Multiscale modeling showing how integrated computation advances lead-free perovskite applications.

2.4. Broader impact and emerging applications

While critical gaps remain, recent advances have firmly established computational tools as central to LFP discovery,[33,69] linking atomic-level insight to device-level performance.[57] From first-principles calculations to high-throughput screening and multiscale modeling, these approaches now support applications beyond photovoltaics, including neuromorphic

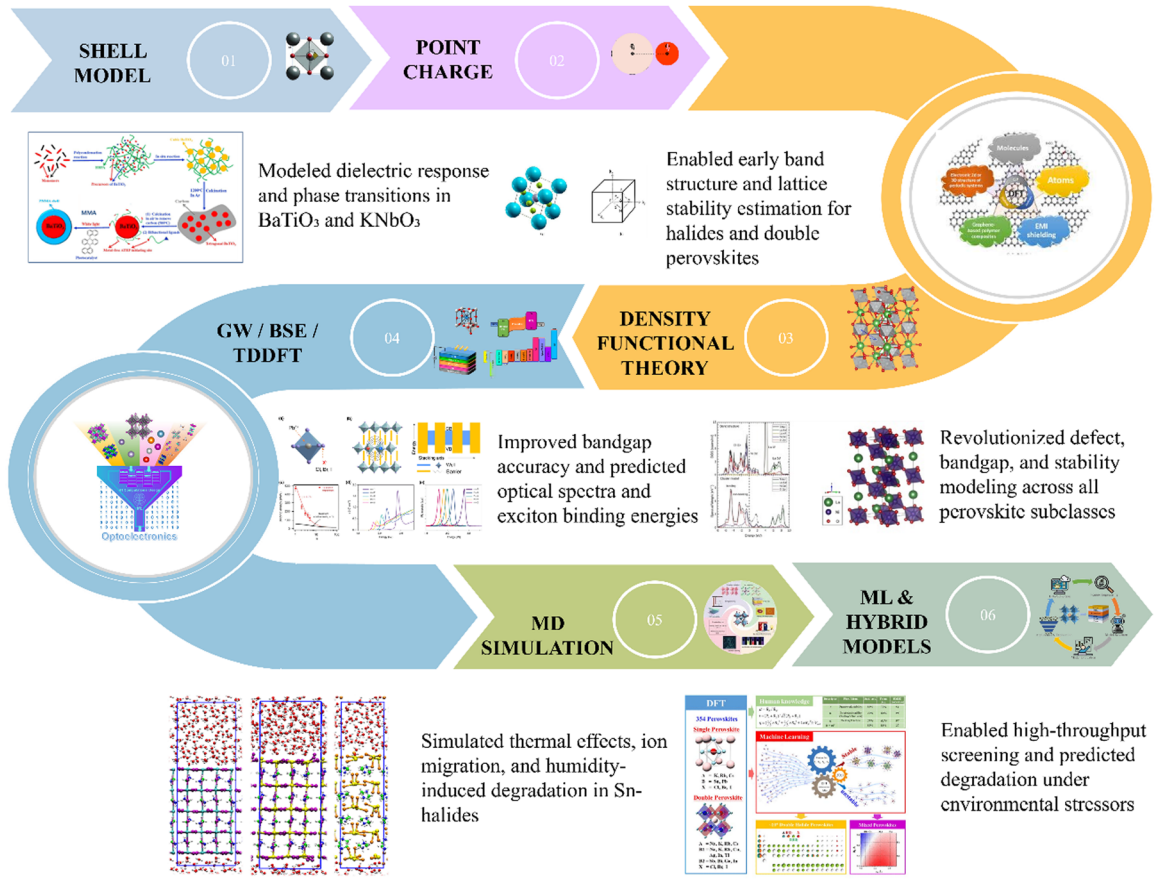

Fig. 5 Schematic timeline illustrating the evolution of computational approaches in LFP research.

Table 1 Milestones in computational methods for lead-free perovskite research

Period	Key developments	Impact	Ref.
Early 2010s	Empirical screening, DFT on Sn/Ge halides	Established early design rules and bandgap estimates	52 and 53
Mid 2010s	Double perovskites, HT-DFT	Enabled prediction and synthesis of $Cs_2AgBiBr_6$	30 and 54
Late 2010s	Inverse design, ML integration	Accelerated screening, broadened applications	55 and 56
2020s	Multiscale modeling, defect physics	Linked atomic-level behavior to device performance	57–59
2020s+	Generative AI, active learning	Autonomous pipelines for multifunctional LFPs	60 and 61

computing,[26] thermal barrier coatings,[21] and scintillators.[23] This shift from isolated property prediction to targeted, application-driven design highlights the growing maturity and versatility of computational strategies in shaping the future of lead-free perovskites.

3. Methodology

3.1. Literature retrieval and search strategy

To systematically collect relevant publications on computational studies of LFPs, we utilized the Publish or Perish (PoP) software[70] in conjunction with the Google Scholar search engine. This approach offers access to a wide range of peer-reviewed articles, conference papers, and institutional repositories, making it suitable for capturing emerging and interdisciplinary research. The main reason for choosing Google Scholar compared to Web of Science and Scopus is that it has many more citations and covers more literature in new and varied fields, as evidenced by the findings of a comparative study.[71] For computational LFP research, this is vital because important achievements are published in many different material science, physics, chemistry, and engineering journals, some of which are not included in both Scopus and Web of Science. PoP supports complex Boolean queries and facilitates bulk export of results in (.ris) format for screening and analysis. Many reference managers use (.ris) files because they are a standard format for sharing reference information between databases. It stores the information in the title, author, publication year, journal, and abstract that can be used in tools such as Zotero and EndNote to filter and edit research papers.

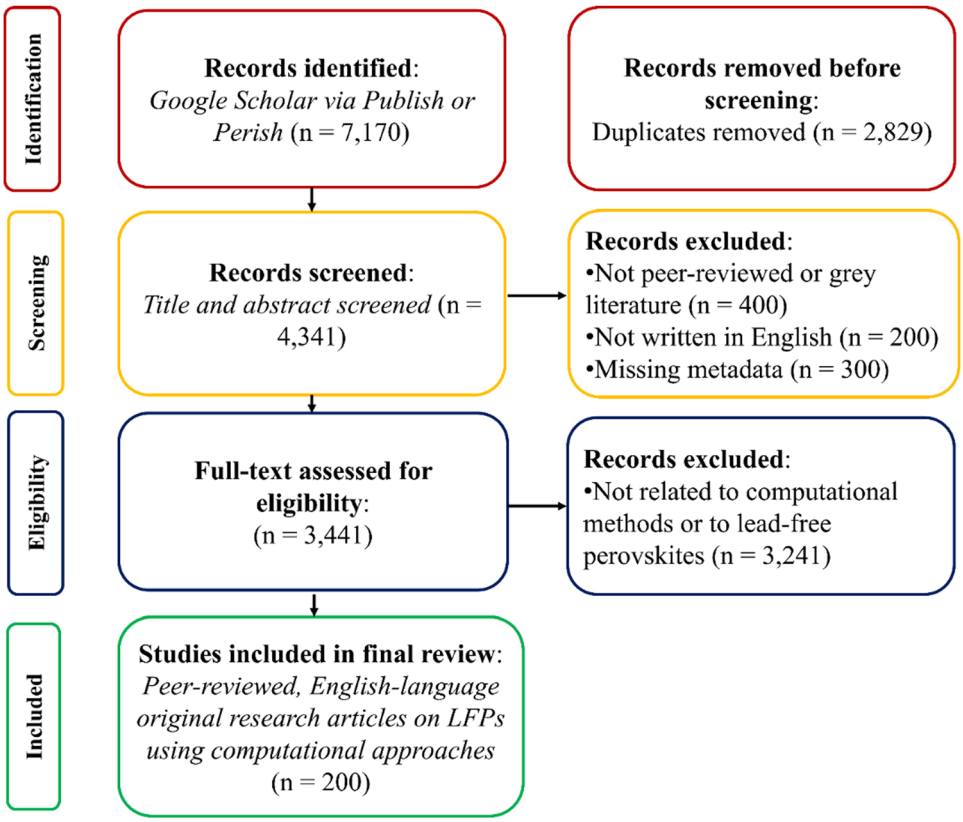

Fig. 6 Document screening and selection process based on PRISMA guidelines.

The search was conducted using a structured Boolean search designed to identify studies that focused on both lead-free perovskites and computational methods. The following search string was used "lead-free perovskite", and (DFT OR "first-principles" OR "machine learning" OR simulation OR computational).

This formula enabled the identification of papers that specifically applied computational techniques to lead-free perovskite frameworks, including first-principles simulations, ML, and other modeling methodologies. The search captured more than ten years of computational advancements in the field, encompassing publications from 2013 to 2025.

3.2. Screening and selection criteria

The screening process was conducted in four stages: identification, screening, eligibility assessment, and inclusion, following the PRISMA (Preferred Reporting Items for Systematic Reviews and Meta-Analyses) framework[72] illustrated in Fig. 6. The overall workflow is illustrated in Fig. 7.

Duplicate entries were first removed using Zotero's built-in duplicate detection tool. Each remaining record was then manually reviewed to assess its relevance based on the title and abstract. Studies unrelated to the objectives of the review, such as those focusing on lead-based perovskites, lacking computational content, or outside the materials domain were excluded.

To ensure transparency in decision-making, we annotated each record within Zotero using tags and notes to indicate the rationale for inclusion or exclusion (*e.g.*, "review article", "conference paper", "no computational method"). Entries that specifically addressed photovoltaic applications were labeled with a "PV" tag during this process. This allowed for efficient identification and deeper analysis of LFP studies focused on photovoltaic performance in later sections. The following inclusion criteria were strictly applied:

- The study must focus on lead-free perovskite materials.
- It must involve at least one computational approach, such as DFT, ML, molecular dynamics, or high-throughput screening.
- It must be a peer-reviewed primary research article (excluding review papers, editorials, preprints, conference papers, book chapters, and books).
- The article must be published in English.

This rigorous filtering process yielded a final dataset of 200 articles, representing a broad and representative sample of computational research in the LFP domain. A smaller subset of representative studies was later selected for detailed discussion in a later section of the review. These were chosen based on methodological depth, application novelty, and relevance to dominant or emerging research themes.

3.3. Metadata processing and analytical framework

Following the screening, the final list of eligible papers was then processed by GROBID (GeneRation Of BIbliographic Data). This is an open-source machine learning tool designed to extract structured bibliographic metadata from scientific

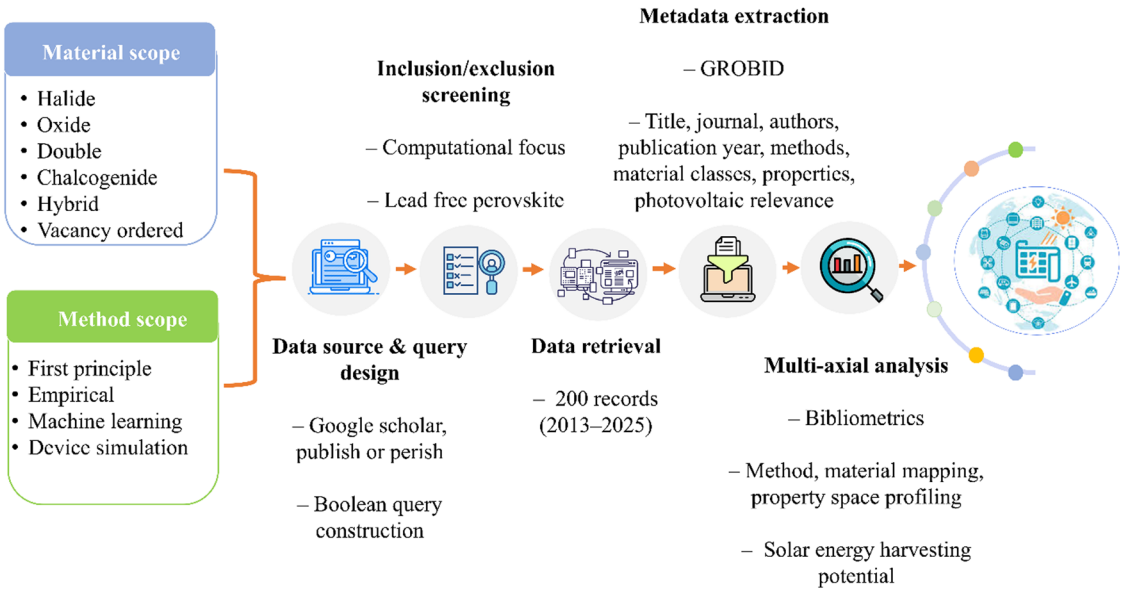

Fig. 7 Overview of the methodological pipeline used in this review.

PDFs.[73] GROBID parsed the documents to extract fields such as article title, authorship, journal name, publication year, and abstract. In addition to core bibliographic fields, domain-specific attributes were manually extracted, including:

- Material class (*e.g.*, halide, oxide, chalcogenide).
- Computational methods used (*e.g.*, DFT, AIMD, ML).
- Software tools, and solvers (*e.g.*, VASP, SCAPS-1D, Quantum ESPRESSO).
- Targeted applications (*e.g.*, photovoltaics, spintronics, thermoelectrics).
- Investigated properties (*e.g.*, bandgap, stability, mobility).

The resulting dataset was consolidated into a metadata spreadsheet and manually reviewed to identify inconsistencies and complete missing entries through full-text verification.

All figures and charts were created using Microsoft Excel, which provided sufficient flexibility and control for generating comparative visualizations. The curated metadata enabled multi-dimensional analysis to uncover key trends in computational LFP research. We assessed publication growth, methodological adoption, tool usage, application diversification, and property-specific focus. A separate subset of photovoltaic studies was further examined to evaluate materials, methods, and tool–property correlations within that domain. Table 2 summarizes the metadata elements extracted and their role in the analysis.

4. Analysis of computational trends in lead-free perovskites

In recent years, computational modeling has become a key driver for the development of lead-free perovskites, underpinning their theoretical foundations, enabling large-scale material screening, and guiding application-oriented design. This section examines the evolution of computational methodologies in LFP research, the factors driving their adoption, and the resulting diversification of applications and material classes.

4.1. Growth of computational studies on lead-free perovskites

Over the past decade, computational investigations of LFPs have expanded markedly, underscoring the growing reliance on theoretical approaches for material discovery and performance prediction. Research activity was limited until 2018, followed by moderate growth through 2020, and a sharp increase from 2023 onwards. The brief decline in 2021–2022 reflected a thematic shift toward broader perovskite systems, and the rapid

Table 2 Summary of metadata elements extracted from selected articles

Metadata field	Purpose of extraction	Use in analysis
Title	Article identification	Manual screening and classification
Journal name	Source credibility and disciplinary scope	Publication source distribution
Year of publication	Temporal context	Year-wise publication trend analysis
Application domain	Functional relevance	Application diversification and domain mapping
LFP subclass	Material categorization (halide, oxide, *etc.*)	Material–application relationship analysis
Computational method used	Identify modeling strategies (*e.g.*, DFT, ML, AIMD)	Method usage and evolution trends
Simulation tool used	Software identification	Tool frequency and specialization analysis
Properties investigated	Target performance metrics	Property-centric trend analysis and tool-property correlation

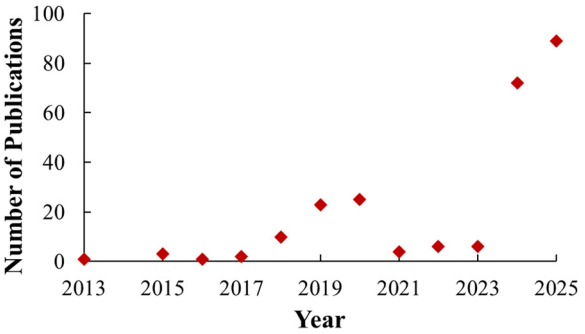

Fig. 8 The annual number of publications of computational LFP research.

adoption of data-driven methodologies, particularly machine learning,[74] rather than a genuine reduction in research output.

During this period, many studies addressed stability in lead-halide perovskites,[75] hybrid perovskite architectures,[76] and tandem device integration.[77,78] Other notable contributions included investigations of energy funneling in hybrid designs[32] and the strengthening of interlayers.[79] While relevant to the broader perovskite field, these topics did not always explicitly feature the ''lead-free'' focus in bibliometric searches.

From 2023, regulatory pressures on lead content and advances in ML-guided discovery of non-toxic alternatives redirected research toward sustainable LFPs, driving a significant rise in publications as depicted in Fig. 8. This growth has been accompanied by increased methodological sophistication, including hybrid functionals, *ab initio* molecular dynamics, ML-assisted workflows, and device-level simulations. Collectively, these developments illustrate the transition of computational modeling from a supplementary tool to a primary driver of innovation in LFP research.

Collectively, these developments illustrate the transition of computational modeling from a supplementary tool to a primary force driving innovation in LFP research, enabled by increasingly powerful and accessible techniques and equipment. This advancement has not only accelerated the pace of discovery but has also expanded the scope of computational studies, allowing for more complex, realistic, and application-oriented modeling of LFP materials.

4.2. Expansion of computational methods and tools

The rapid increase in computational research of perovskites without lead is directly related to the development and expansion of the available methodologies and tools. These advancements have progressively allowed researchers to address a broader range of material challenges with increasing accuracy, from electronic structure and stability to thermodynamic behavior and device performance.

4.2.1. Density functional theory. DFT is one of the most fundamental methods that enabled the progress of LFPs. It was in the 1960s when Hohenberg and Kohn[80] introduced the basic ideas of DFT, which Kohn and Sham[81] then expanded to cope with many-electron systems, and their total energy. Following improvements in algorithmic and computing technologies, this transformation greatly cut down the computing time, and appeared in the 1990s.[82,83] Even without using experimental results, DFT can precisely predict total energy, the structure of the electrons, and where the positive charges are located, as explained by Becke.[84] Due to its resilience and adaptability, it is the preferred approach in computational materials science, especially when researching novel materials like LFPs.[85,86] Due to the development of practical tools such as WIEN2k and VASP software, DFT became a standard method among scientists. Blaha *et al.*[87] introduced WIEN2k with the FP-LAPW method, and this software is renowned for accurately depicting periodic solids. In an alternative tool VASP, first developed by Kresse and Furthmüller,[88] plane-wave basis sets and pseudo-potentials are used, and the software contains extra options for molecular dynamics and better exchange–correlation functions. DFT is important in computational materials science mainly because of these valuable tools. By applying simulations, scientists can now carefully forecast which lead-free perovskites are stable, what energy states they exhibit, and how they compare in terms of bandgap. This has helped to identify and optimize environmentally friendly substitutes for lead-based materials.[86,89] For example, Taylor *et al.*[90] laid the groundwork for further computational investigation by investigating the structural and electronic properties of perovskites using semi-local DFT with WIEN2k. As shown in Fig. 9a, DFT is the most consistently used method across all years. Fig. 9b confirms the significant role of WIEN2k and VASP, which appeared to be the most frequently used software in the entire dataset.

4.2.2. Beyond standard DFT. Although DFT offers a solid basis, its conventional applications have known drawbacks, particularly when describing materials with localized d and f orbitals or strongly correlated electrons.[91,92] These shortcomings frequently show up as inaccurate magnetic ordering, an underestimation of band gaps, or a poor description of charge localization. Corrective techniques like DFT+U, which penalize on-site Coulomb interactions with a Hubbard-like correction, and hybrid functionals, which incorporate a fraction of exact exchange from Hartree–Fock theory, have been developed and widely used to address these shortcomings.[93] These methods gained attention as researchers worked to improve electronic property computations for more precise modeling of perovskite semiconductors and related materials. Fig. 9a shows that DFT+U is used sparingly but consistently, mainly from 2018 to 2020. Its moderate presence indicates that, despite their value, these corrections are only used in systems where traditional DFT is insufficient.

The application of *ab initio* molecular dynamics (AIMD) was another significant advancement. By simulating atomic motion at finite temperatures, AIMD makes it possible to investigate thermal stability, phase transitions, and defect migration.[94] Its use in lead-free perovskite research has allowed dynamic property predictions beyond the static ground-state results of standard DFT.[89,95] For example, Gupta *et al.*[96] used AIMD to examine phase stability in $BaZrS_3$, providing insight into structural resilience under thermal conditions. However, due to its

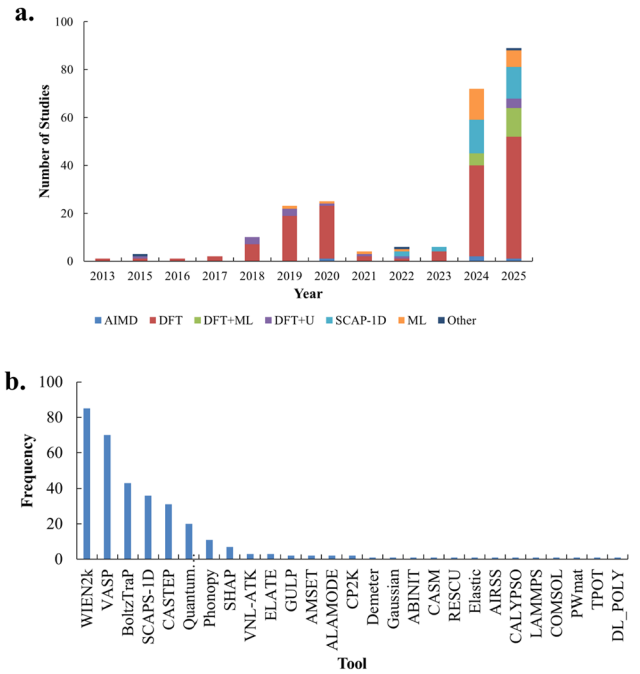

Fig. 9 (a) Year-wise trends in the adoption of computational methods in LFP studies showing increasing methodological diversification. (b) Frequency of simulation tools used, highlighting dominant platforms and emerging specialized tools. The data shown is based on manual extraction from 200 peer-reviewed studies included in this review.

computational cost, AIMD remains less commonly used. As shown in Fig. 9a, AIMD appears infrequently, with activity concentrated in periods where detailed thermal analysis was a primary research focus.

As an interest in specific functional properties increased, additional tools emerged to support phonon and thermoelectric calculations.[97] Phonopy, released in the late 2000s, provides a DFT-compatible framework for phonon dispersion analysis, essential for evaluating vibrational stability. Haque and Hossain[98] used Phonopy to study lattice dynamics and stability in perovskite systems, contributing to the growing adoption of vibrational analysis tools. BoltzTraP, developed in 2006, enables semi-classical Boltzmann transport calculations using DFT-derived electronic structure data. It has been used in thermoelectric modeling to predict electrical conductivity and Seebeck coefficients. For example, Sharma *et al.*[99] applied BoltzTraP to assess thermoelectric behavior in perovskites, illustrating the increasing alignment between method and material functionality. As shown in Fig. 9b, BoltzTraP is the second most frequently used tool, indicating its strong role in thermoelectric modeling. Phonopy also appears prominently, especially in studies conducted after 2018.

4.2.3. Machine learning and multiscale modeling. With the introduction of machine learning into the computational materials space, the field has recently moved toward data-driven approaches. Once trained on appropriate datasets, machine learning models can quickly predict material properties by recognizing intricate patterns in high-dimensional chemical and structural spaces.[34,42] This has proven particularly useful for designing LFPs, enabling the screening of candidates with desired optoelectronic or structural characteristics, thus accelerating discovery.

For example, Zou *et al.*[100] demonstrated efficiency gains with hybrid workflows, performing high-throughput screening of perovskite compositions using a DFT+ML pipeline. Fig. 9a shows a sharp increase in ML and DFT+ML applications after 2023. Libraries such as XGBoost and TPOT facilitate model training, feature selection, and optimization, while the inclusion of SHAP in recent studies reflects the growing interest in interpretability and explainable AI.

Multiscale integration is evident in the growing use of SCAPS-1D for photovoltaic device modeling.[101] Researchers use SCAPS-1D to relate device-level performance metrics, such as efficiency and current–voltage behavior, to materials-level characteristics like band alignment and defect density. Shoab *et al.*,[102] and Ravidas *et al.*[103] combined SCAPS-1D with DFT to model lead-free perovskite solar cells, bridging the gap between atomistic simulations and real-world devices. Fig. 9a also shows the emergence of SCAPS-1D after 2023, particularly in studies integrating materials modeling with solar cell simulation.

Other specialized tools appear less frequently, focusing on niche applications such as lattice dynamics or classical force-field simulations. While they add diversity, their lower adoption suggests a narrower scope or competition from more established platforms.

These developments illustrate how the expansion of computational methods and tools has shaped the research landscape. The timeline reflected in Fig. 9a shows not just growth, but diversification, moving from single-method studies to integrated, property-targeted workflows. While DFT remains the central framework, its combination with machine learning, transport analysis, and device simulation has enabled more comprehensive and application-driven exploration of lead-free perovskites.

4.3. Computationally driven diversification of LFP applications

With the increasing methodological depth and tool accessibility discussed in the previous section, an important question naturally emerges regarding the purpose of these computational approaches. Our analysis shows that the expansion of computational capabilities has directly enabled the exploration of LFP across a broad and growing range of application domains. As illustrated in Fig. 10, computational studies on LFPs were initially concentrated in the photovoltaic domain. Beginning around 2019, however, the field experienced a steady thematic expansion. More recent years have witnessed a significant increase in studies targeting photocatalysis, thermoelectrics, spintronics, neuromorphic computing, scintillators, and thermal barrier coatings. This trend reflects the adaptability of LFP chemistries and the increasing ability of computational models to evaluate application-specific performance metrics.

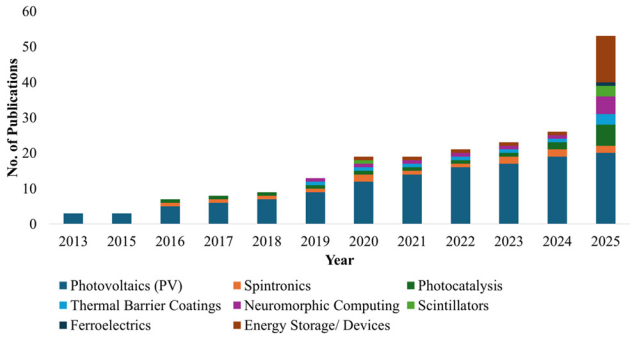

Fig. 10 Thematic evolution of LFP applications in computational studies.

4.3.1. Photocatalysis. Photocatalysis emerged as one of the earliest non-photovoltaic applications explored for lead free perovskites. Studies in this area typically employ hybrid DFT methods to assess band edge positions, redox alignment, and light absorption properties. For instance, Rehman *et al.*[25] screened Dion–Jacobson perovskites like $RbCa_2Ta_3O_{10}$ with the HSE06 functional, and they obtained favorable activity for water splitting under the sun. Xiao *et al.*[104] also achieved visible-light-induced oxidative photocatalysis *via* halide lead-free perovskites with the appropriate bandgaps and electronic structure for the formation of reactive oxygen species.

4.3.2. Energy devices. Energy devices have very recently emerged as one of the fastest-growing domains for LFPs, as reflected by the sharp rise in publications in 2024–2025 (Fig. 10). Computational studies in this space depend extensively on the use of applications like BoltzTraP and Phonopy to analyze the Seebeck coefficients, electrical conductivity, and thermal conductivity of the lattice. Sharma *et al.*[99] obtained a *ZT* of ~1.06 in doped $CsZnBr_3$, whereas Haque and Hossain[98] indicated the same promise in $Cs_2InAgCl_6$, demonstrating the capability of halide LFPs compared to conventional thermoelectric materials.

4.3.3. Spintronics. Spintronics has emerged as a promising but relatively less explored application of lead-free perovskites, with a steady increase in computational studies in recent years (Fig. 10). Techniques such as DFT+*U* and AIMD are frequently applied to evaluate magnetic ordering, band structure, and spin-polarized states. Quraishi *et al.*[105] reported that $TlTiBr_3$ exhibits half-metallic behavior with strong spin polarization, highlighting the potential of halide LFPs in next-generation spintronic devices.

4.3.4. Neuromorphic computing. Neuromorphic computing applications of LFPs have also gained much attention, particularly in the context of resistive switching and ion migration, as reflected in the growing publication trend (Fig. 10a). Computational tools such as the nudged elastic band method are employed to probe migration barriers, while AIMD simulations help uncover dynamic switching mechanisms. Zhang Zizi *et al.*[106] for example, showed that $CsAg_2I_3$ possesses low migration barriers for Ag^+, and I^- ions, enabling analog resistive switching characteristics desirable for neuromorphic devices.

4.3.5. Radiation detection and thermal applications. Radiation detection and thermal applications, such as thermal barrier coatings, have seen growing attention in recent years. Computational analyses often employ phonon dispersion and elastic constant calculations, as well as AIMD, for the analysis of thermal robustness and vibrational stability. Rahman *et al.*[107] identified Ba_3SbI_3, a material with low thermal conductivity, for its potential application as a thermal barrier coating, while $BaMnO_3$ also demonstrated promising thermal properties. In contrast, $CaMnO_3$ was noted for superior high-temperature resilience due to its higher melting point and Debye temperature.[108] These findings highlight the versatility of LFPs for thermal protection applications.

An overview of these diversified application domains is presented in Fig. 11, which illustrates the expanding reach of LFPs across energy, optoelectronic, neuromorphic, and radiation-sensitive technologies. This diversification has been driven by the integration of computational tools with property-specific evaluation strategies, enabling rapid screening and targeted optimization across a broad spectrum of use cases.

4.4. Cross-domain property trends

Beyond application-specific studies, it is equally important to consider the broader trends in material properties that underpin multiple domains. Fig. 12 represents the frequency of studied properties across all LFP applications. Bandgap and optical absorption dominate, reflecting their central role in energy conversion processes and their necessity for screening materials for photovoltaic, photocatalytic, and related optoelectronic applications. Dielectric properties, Seebeck coefficients, and phonon-related descriptors are also prevalent, aligning with the demands of optoelectronic, thermoelectric, and thermal barrier coating applications.

At the same time, less frequently investigated properties such as defect tolerance, exciton binding energy, and spectroscopic limited maximum efficiency, highlight a shift toward more targeted, application-specific modeling approaches. These descriptors are often critical for advanced device optimization but require greater computational sophistication. For instance, Vicent-Luna *et al.*[110] employed the GFN1-xTB method to efficiently compute electronic band structures and density of states in halide perovskites, offering a low-cost alternative to DFT for large-scale computational screening.

4.5. Mapping applications to material classes

While property trends highlight common computational descriptors across applications, another important perspective comes from examining how specific material subclasses of LFPs are linked to targeted functionalities. A clear stratification emerges across halide, oxide, double perovskite, and vacancy-ordered systems, reflecting the way intrinsic chemistry and structural motifs shape device relevance. This mapping underscores that advances in computational methodology are not only broadening the scope of applications but also deepening the material–function relationship. As highlighted earlier, LFPs can be classified along multiple overlapping dimensions, including anion chemistry, dimensionality, bonding character, and B-site configuration (Fig. 1). The present analysis, as shown

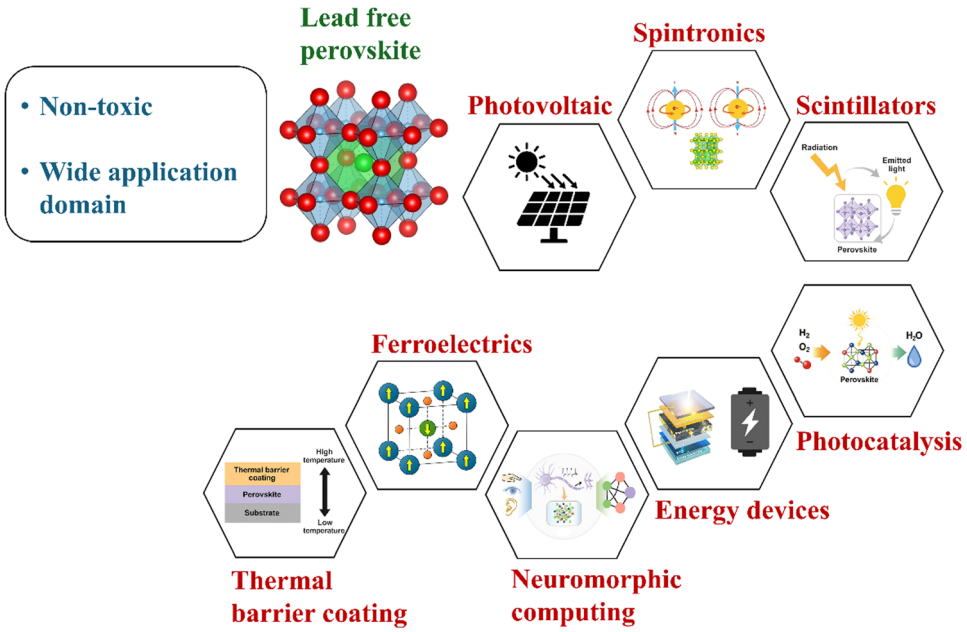

Fig. 11 Overview of major application domains explored using computational modeling of LFPs.

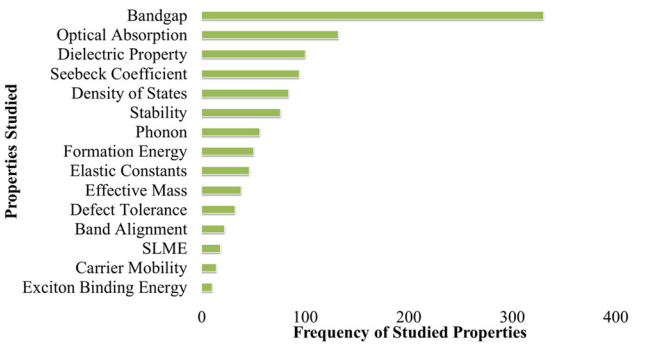

Fig. 12 Frequency of properties investigated across computational LFP studies.

in Fig. 13(a and b), emphasizes B-site classification showing how different subclasses are preferentially studied for distinct device paradigms.

4.5.1. Double perovskites. Double perovskites are the focus of extensive computational research as shown in Fig. 13a, particularly in diverse applications such as photovoltaics, optoelectronics, photocatalysis, and spintronics. Their chemical flexibility allows for precise tuning of bandgap, stability, and magnetic behavior. For instance, $Cs_2AgBiBr_6$ has been widely studied for PV and photodetector applications due to its indirect bandgap and robust environmental stability.[111,112] In spintronic contexts, $TlTiBr_3$ and Sr_2SnMnO_6 have shown potential due to their spin-polarized electronic structures and ferromagnetic behavior.[105,113]

4.5.2. Halide perovskites. Halide LFPs represent another major subclass with broad application coverage across photovoltaics, LEDs, thermoelectrics, and optoelectronics (Fig. 13a). Their appeal lies in highly tunable optoelectronic properties combined with low-temperature processability. Tin and Cu-based halides have been widely studied for photovoltaics, benefiting from tuneable optoelectronic properties and low-temperature synthesis, while neuromorphic functionalities have also been demonstrated. $CsAg_2I_3$ shows neuromorphic functionality *via* double-ion diffusion and low-threshold conduction, and compatibility for photonic applications.[26] Moreover, hybrid DFT calculations at the B3LYP/6-311++G(d,p) level confirmed the ability of halide LFPs to drive visible-light oxidative photocatalysis through singlet oxygen and superoxide formation,[104] further extending their multifunctional potential.

4.5.3. Oxide perovskites. Oxide LFPs are most prominently represented in "other" applications such as thermal barrier coatings and catalysis. Their suitability arises from strong phonon scattering, high melting points, and robust chemical stability, which enable performance under extreme conditions. For example, $BaMnO_3$ demonstrates strong UV absorption and intrinsically low thermal conductivity, making it attractive for turbine environments.[108] Similarly, Ba_3SbI_3 combines dynamic stability, UV responsiveness, and low thermal conductivity, reinforcing its potential for high-temperature coating applications.[107]

4.5.4. Other material classes. Beyond halide and oxide systems, several additional subclasses of LFPs are beginning to expand their presence across diverse applications, though at a smaller scale as shown in Fig. 13a. Hybrid organic–inorganic perovskites have found use primarily in LEDs and solar cells, with $CH_3C(NH_2)_2SnI_3$ identified through machine learning screening as a promising candidate due to its 1.87 eV bandgap and low defect density.[114] Chalcogenide perovskites represent another emerging direction, exemplified by Ba_2BiNbS_6, which has been proposed as a stable lead-free PV absorber

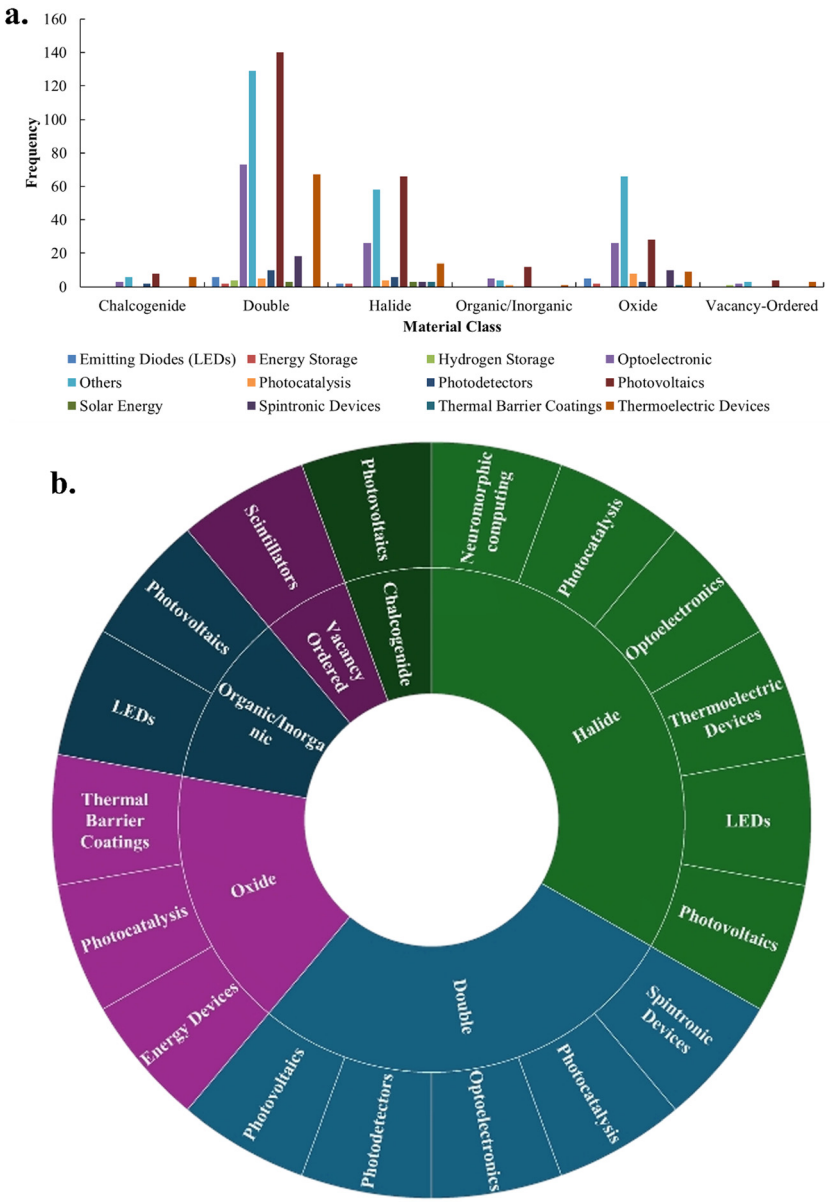

Fig. 13 (a) Frequency distribution of major application domains across LFP material classes based on B-site configuration. (b) Sunburst chart illustrating functional mapping from material classes to application domains, highlighting multifunctionality, and cross-domain relevance.

with near-zero decomposition energy.[115] Vacancy-ordered systems also show growing potential, as demonstrated by Ba_2SnBr_4, investigated as a scintillator with tunable radioluminescence properties.[109] These examples demonstrate how diverse chemical classes of LFPs are being computationally tailored to specialized device contexts.

4.6. Structure–function mapping

A key outcome of computational expansion is the ability to directly link material subclasses with targeted application domains. The mapping in Fig. 13b demonstrates how computational screening aligns material class with application needs, leveraging LFP chemistry versatility. It confirms oxides are being investigated for high-temperature and mechanical applications, even though double perovskites and halides are still essential to photovoltaics and optoelectronics. The compatibility of LFP chemistries and the effectiveness of computational screening in focusing research are both demonstrated by the alignment of material class and application needs.

This section demonstrates how modeling and simulations have taken center stage in the study of LFPs, offering crucial insights into their stability, structure, and potential for real-world use. Starting from early studies using density functional theory,[90,116] the field has grown to include more advanced techniques such as *ab initio* molecular dynamics,[96] hybrid functionals,[25] transport modeling,[99] and machine learning approaches.[100] These resources have aided researchers in investigating a wider range of applications in addition to

understanding the fundamental characteristics of materials. The initial emphasis on photovoltaic devices has since paved the way to a more comprehensive investigation of lead-free perovskites in a variety of functional areas. Because of their compositional flexibility and ease of simulation, double perovskites and halides are the most common. However, the discovery of other promising types may be limited by this intense focus on well-known materials. Subclasses that are less prevalent, including vacancy-ordered perovskites and chalcogenides,[109,115] are still not studied as much, often because of limited data or higher computational cost. Most simulations are based on ideal conditions, defect-free structures, and do not accurately represent real-world circumstances, such as temperature effects or device interfaces. This is another significant drawback. While some studies have addressed these issues using more realistic simulations,[96,106] they remain relatively few. Overall, the progress in computational tools has made it possible to screen materials faster and design them more precisely. However, future work should aim to include a wider variety of material classes, simulate more realistic conditions, and work more closely with experimental validation. This will help ensure that computational research continues to guide the discovery of safer, more efficient lead-free perovskites for next-generation technologies.

5. Lead-free perovskites for photovoltaic applications

5.1. Growth and drivers of photovoltaic-focused LFP research

Among all the emerging application domains, photovoltaics stands out as the most extensively explored and methodologically mature area within the computational study of LFPs. This maturity is marked not only by the volume of published work (156 studies on the photovoltaic potential of LFP) but also by the completeness of the computational pipelines employed. As computational methods have advanced, photovoltaic-focused studies have transitioned from simple bandgap predictions to comprehensive workflows that integrate materials modeling, property analysis, and full-stack device simulation. As illustrated in Fig. 14, the number of computational studies on LFPs for photovoltaic applications has grown steadily over the past decade, with a significant surge beginning in 2023. The surge in 2023 can be attributed to advances in machine learning, regulatory pressure to replace toxic lead, and the emergence of high-performing lead-free candidates. Cai *et al.*[117] screened ~12 million compounds using a physics-informed ML model, identifying 17 stable materials with >20% predicted efficiency. Hu and Zhang[118] combined DFT and ML to discover new 2D lead-free perovskites with optimized band gaps and thermodynamic stability. These innovations, alongside initiatives like the EU-funded SUNREY project, significantly accelerated computational efforts in this field. This rise reflects both the urgency of finding stable and non-toxic alternatives to Pb-based perovskites and the increasing confidence in computational techniques to deliver reliable pre-screening and device-level predictions.

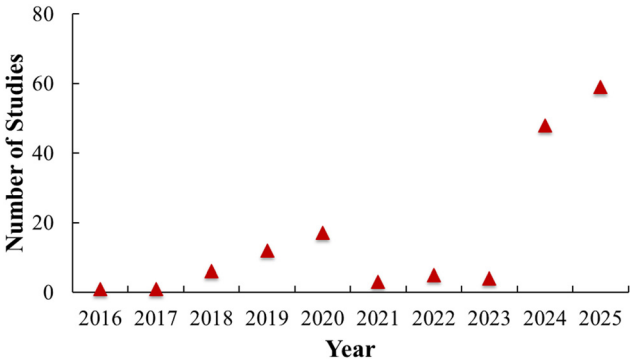

Fig. 14 Photovoltaic-focused analysis of computational LFP studies illustrating growth in PV-relevant publications over time.

5.2. Material classes and their photovoltaic potential

The distribution of material classes in photovoltaic-focused studies shown in Fig. 15 highlights the dominance of double perovskites (43%) and halides (23%), reflecting their versatility and suitability for solar energy conversion. Oxides account for a smaller but still substantial fraction (19%), while organic/inorganic, chalcogenide, and vacancy-ordered systems remain comparatively underexplored. This stratification underscores how computational pipelines are increasingly directed toward classes that balance tunable optoelectronic properties with chemical stability.

Double perovskites stand out not only for their prevalence but also for their performance in critical photovoltaic descriptors, including optimal band gaps, defect tolerance, and stability. $Cs_2AgBiBr_6$ exemplifies this class, combining low toxicity and ambient durability with a tunable indirect bandgap. Ji *et al.*[119] demonstrated that its bandgap could be reduced from 1.98 eV to 1.72 eV through temperature-controlled synthesis, attributing the shift to Ag–Bi disorder confirmed by DFT. Saifee *et al.*[120] further advanced this by reporting a ~1.6 eV bandgap with strong environmental resilience, emphasizing the material's viability for device integration.

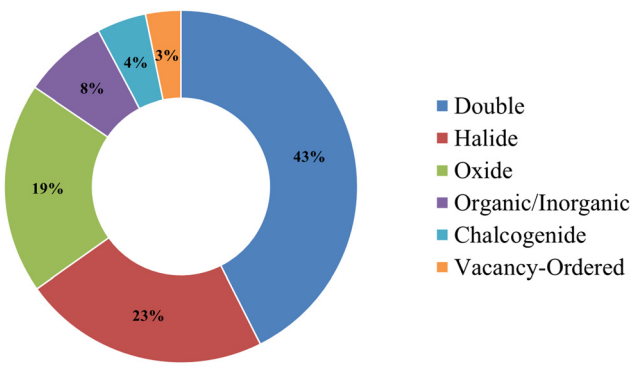

Fig. 15 Material class distribution in photovoltaic studies.

Halide perovskites, meanwhile, continue to attract attention for their superior optical properties and compatibility with thin-film fabrication. Riaz *et al.*[121] showed that $CsEuBr_3$ meets key benchmarks for solar absorbers, with a suitable 1.2 eV bandgap and strong light absorption capacity, making it a strong candidate for efficient solar energy harvesting.

Although smaller in share, oxides and other subclasses contribute to diversifying the materials landscape. Their presence indicates an emerging interest in expanding beyond the well-established double and halide systems, suggesting future opportunities for discovery once computational and experimental pipelines mature further.

5.3. Key performance-related properties targeted in modeling

A distinguishing feature of photovoltaic research in LFPs is the strong emphasis on performance-relevant properties. As shown in Fig. 16a, bandgap calculations remain central, followed by extensive focus on fill factor, optical absorption, dielectric properties, and device-relevant metrics such as open-circuit voltage and power conversion efficiency. The emphasis on bandgap highlights its crucial role in determining the suitability of a material for photovoltaics, with numerous studies identifying compounds in the 1.3–1.5 eV range as optimal, in line with the Shockley–Queisser limit. To cite an example, Jain *et al.*[119] performed a high-throughput analysis regarding optimum bandgaps, and Shoab *et al.*[102] and Rahman *et al.*[107] evaluated the fixed-bandgap perovskites $MASnI_3$ and Ba_3SbI_3, respectively, which incidentally both lie in the optimum spectral response.

The focus on fill factor and open-circuit voltage is a growing trend towards prediction rather than material screening alone. For instance, predictions of theoretical FF, V_{oc}, and PCE for various $RbSnX_3$ absorber layers were made by Ravidas *et al.*[103] using DFT with the help of SCAPS-1D simulations, evidencing the transition towards device-aware modeling protocols in lead-free perovskites. Optical absorption is a routine metric in halide perovskite studies because of their large extinction coefficients, and visible-light band alignment, aspects used in high-throughput screening studies such as Xiao *et al.*[104]

5.4. Linking material classes to ideal photovoltaic properties

This focus on performance is further reinforced when material class is mapped to the number of ideal photovoltaic properties each exhibits (Fig. 16b). Double perovskites exhibit the highest count, particularly in optimal band gaps, defect tolerance, and stability. $Cs_2AgBiBr_6$ exemplifies this class with low toxicity, ambient durability, and a tuneable indirect bandgap. Ji *et al.*[112] reduced its bandgap from 1.98 eV to 1.72 eV *via* temperature-controlled synthesis, attributing the shift to Ag–Bi disorder confirmed by DFT. Saifee *et al.*[120] further reported a ~1.6 eV bandgap and strong environmental resilience. Halide systems such as $CsEuBr_3$, with proven capability to meet key optical and electronic property benchmarks, including a suitable 1.2 eV band gap and strong light absorption, show significant promise for solar energy harvesting.[121]

5.5. Computational toolchain for photovoltaic LFP studies

The methodological maturity of photovoltaic-focused LFP research is underpinned by a well-established computational toolchain ecosystem. As shown in Fig. 17, WIEN2k remains dominant for bandgap calculations, benefiting from the TB-mBJ potential's improved accuracy over conventional DFT methods. Optical absorption is also frequently studied using WIEN2k, and SCAPS-1D, the latter playing a central role in linking atomistic properties with macroscopic device metrics such as current–voltage behavior and maximum power output. VASP is heavily utilized for formation energy, defect tolerance, and effective mass analysis, leveraging its robust plane-wave basis and extensive pseudopotential database. Phonon calculations are vital for assessing thermal stability, and phonon modes are typically carried out using Phonopy and Quantum ESPRESSO. Spectroscopic limited maximum efficiency (SLME), a lesser-known but increasingly used performance factor for

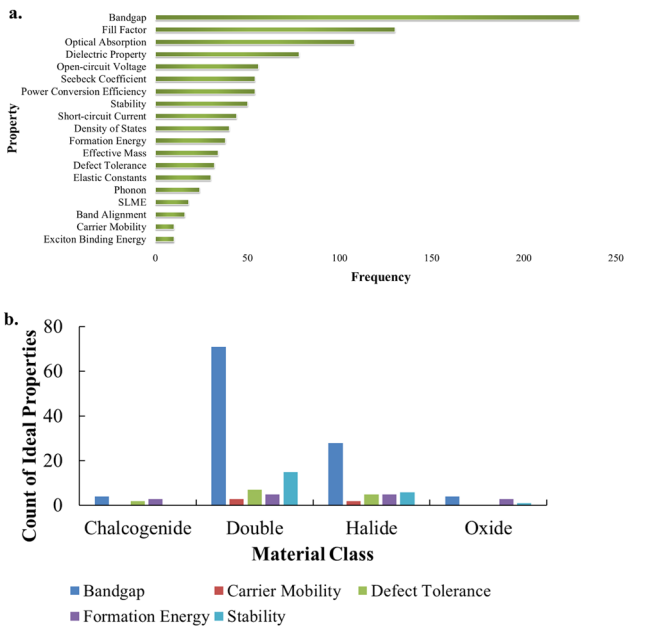

Fig. 16 (a) Frequency of properties targeted in PV modeling and (b) ideal property count across material classes.

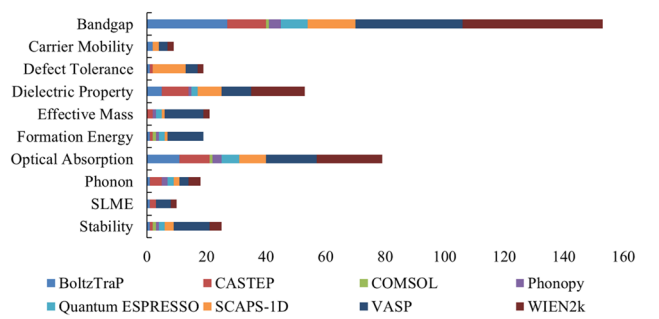

Fig. 17 Mapping of computational tools to properties studied in photovoltaic applications.

photovoltaics, was applied in their studies with an application explicitly oriented towards intrinsic light principles.[115]

5.6. Towards end-to-end computational workflows

Advances in modeling and simulation now allow researchers to construct complete computational narratives of material behavior, from stability and optical response to device-level performance. Researchers are no longer constrained from asking questions about whether a material might be stable or might be optically active. Instead, researchers are constructing end-to-end narratives of material performance. These workflows not only identify stability and functionality but also reveal limitations and provide guidance for design enhancement through compositional optimization and process refinement. Photovoltaics thus serves as a model domain, where theory-driven screening, multiscale modeling, and integrated toolchains converge to accelerate the development of lead-free perovskite materials with improved efficiency, durability, and scalability.

6. Emerging patterns and future directions

6.1. Transition to application-oriented research

The area of computational lead-free perovskites is transitioning from the early discovery phase to application-driven development. As illustrated throughout this review, the advances in computational tools and techniques have not only expedited the screening of materials but also facilitated targeted investigation of LFPs across various applications, including spintronics, photovoltaics, photocatalysis, and thermal barriers. The field of computational LFP is steadily advancing from exploratory material discovery toward application-driven, methodologically sophisticated research. As shown in Table 3 and discussed throughout Section 4, this evolution is marked by tighter integration between computational strategies, material subclasses, and functional objectives.

This development reflects the rapid growth of computational studies in recent years, enabled by a proliferation of accessible electronic structure codes, transport models, and machine learning (ML) toolkits (Section 4). Halide and double perovskites remain the most intensively studied subclasses, driven by their structural tunability and strong optoelectronic performance. Photovoltaics, in particular, continues to dominate the application landscape, with numerous studies combining DFT, Boltzmann transport theory, and SCAPS-1D device simulations to model absorber properties, carrier dynamics, and power conversion efficiency, as discussed in Section 5. Examples include the simulation of 29.41% PCE for Rb_2AlAgI_6,[122] and 33.84% for Cs_2TiBr_6-based solar cells,[123] which underscore the growing predictive capability of computational design frameworks.

6.2. Recurring research methodologies across domains

An important observation emerging from Table 3 is the recurrence of research teams applying consistent methods across diverse applications. For example, Nazir *et al.*[124–126] have systematically employed DFT and BoltzTraP to investigate double perovskites across photovoltaic, thermoelectric, and optoelectronic domains. Similarly, Zhang Zizi *et al.*,[106] Zhang Zhaosheng *et al.*,[114] and Zhang L. *et al.*[18] have used machine learning–augmented DFT workflows to explore photovoltaic and photocatalytic functionalities. Reza *et al.*[123,127] applied device simulations to halide perovskites across different architectures, indicating growing methodological continuity across material systems.

Simultaneously, photovoltaics is being modeled using a wide variety of LFP chemistries, not just halide perovskites,[127–129] but also double perovskites,[106,120,130] oxide perovskites,[131] chalcogenide perovskites,[132] and hybrid organic–inorganic perovskites.[133,134] This trend, detailed in Section 4, demonstrates the material adaptability of the perovskite framework to support diverse optoelectronic applications.

In parallel, certain material classes are being deployed across multiple functional domains, further reinforcing their versatility. Double perovskites serve in photovoltaics, thermoelectrics,[135,136] stability screening,[100,137] spintronics,[90] photocatalysis,[138] and CO_2 catalysis.[139] Oxide perovskites are similarly used in photovoltaics,[131] thermoelectrics,[140] spintronics,[141] gas sensing,[142] and ferroelectricity.[116] These cross-functional deployments highlight the increasingly modular and transferable nature of LFP computational workflows.

Diverse approaches are becoming more similar due to recent advancements in research methodology. While SCAPS-1D has emerged as a key tool for modeling photovoltaic devices,[120,129] WIEN2k + BoltzTraP has become a standard toolkit for modeling thermoelectric, and optical transport. At the same time, property prediction is accelerated, structural descriptors are interpreted, and device configurations are optimized with machine learning tools such as CatBoost, XGBoost, LightGBM, and symbolic regression. Surrogate models like the orthorhombic structure predictor,[143] and custom frameworks like ECSG[100] are examples of attempts to boost computational efficiency without sacrificing physical interpretability.

Defect tolerance and structural stability modeling, which are crucial for long-term device performance, are another new area of interest, as established earlier in Section 5. Defect formation energy, and passivation behavior are directly incorporated into material screening in studies like Zhang Zhaosheng *et al.*[114] and Yun *et al.*[128] Similarly, interpretable, generalizable descriptors of thermodynamic stability are constructed using ML frameworks such as those by Shi *et al.*[133] and symbolic regression.[137]

6.3. Advanced design strategies for property optimization

Strain engineering,[106] dimensional control,[128] and site mixing[134] are recurring design approaches observed in materials and applications. They are increasingly applied to modify bandgaps, enhance carrier mobility, or mitigate defect states. To maximize performance across composition and device architecture, these tactics are frequently combined with high-

Table 3 Representative computational studies of lead-free perovskites

LFP type	Application studied	Method used	Computational tool used	Key concept	Ref.
Double perovskite	Stability prediction and materials discovery	ML + DFT	Electron configuration models with stacked generalization (ECSG) ensemble, including electron configuration convolutional neural network (ECCNN) + VASP	Developed a custom ensemble ML framework (ECSG) incorporating electron configuration to enhance stability prediction and discover new wide-bandgap materials with high data efficiency	100
Double perovskite	CO_2 splitting, and industrial decarbonization	MD + thermodynamic modeling + experimental	LAMMPS + COMSOL multiphysics	Demonstrated $Ba_2Ca_{0.66}Nb_{0.34}FeO_{6-\delta}$ (BCNF) as an efficient CO_2-splitting catalyst enabling closed-loop carbon recirculation in steelmaking, operating at 700–800 °C with significant emission reduction, and industrial scalability	139
Double perovskite	Photovoltaics	ML + DFT + Device Simulation	Random forest, gradient enhanced regression, support vector machine regression, ridge regression, extreme gradient boosting + CASTEP + SCAPS-1D	Developed a machine learning-guided design framework to identify $Cs_2AgSbCl_6$ as a strain-tolerant double perovskite light absorber. Demonstrated that micro-strain tuning enables mechanical flexibility, thermal stability, and preserves optoelectronic performance, achieving 21.38% simulated photovoltaic efficiency	106
Hybrid organic–inorganic perovskite	Photovoltaics	ML + DFT	XGBoost, LightGBM, CatBoost, random forest, CustomCNN, VGG16, xception, EfficientNetV2B0, GCSConv, GCNConv, GATConv + VASP	Developed an ML-assisted high-throughput framework using advanced structural descriptors and 11 algorithms to screen hybrid perovskites. Identified $CH_3C(NH_2)_2SnI_3$ as a lead-free candidate with strong defect tolerance and high potential photovoltaic performance	114
Oxide perovskite	Photocatalytic water splitting	ML + DFT	TPOT + VASP	Used TPOT automated ML to screen 5329 ABO_3 perovskite oxides for photocatalytic band edge properties. Achieved 42% error reduction *via* ensemble learning. Identified 57 candidate materials for water splitting, validated with VASP	18
Halide perovskite	Neuromorphic computing	DFT + simulation + experimental	VASP + Custom ANN	Developed a lead-free halide perovskite analogue ($CsAg_2I_3$) memristor with HI-induced interstitial doping to enable dual-ion migration, and analog resistive switching, achieving stable synaptic plasticity, and 93% image recognition accuracy for neuromorphic computing applications	26
Mixed perovskites (oxide perovskites, oxynitride perovskites, Ruddlesden–Popper perovskites)	Photovoltaics	ML	CatBoost, gradient boosting	Developed an ML-based framework using Matminer features and Materials Project data to predict bandgap properties of diverse perovskites for photovoltaic applications. Gradient Boosting achieved the highest AUC (0.864) with stability considered. SHAP and LIME revealed key structural and compositional factors	144
Oxide perovskite	Thermal barrier coatings (TBCs)	AIMD + ML Potentials + Classical MD + PIMD + HNEMD	VASP + MLIP + LAMMPS + GPUMD	Developed a multi-method computational framework integrating AIMD, machine-learned interatomic potentials, and classical/quantum molecular dynamics to identify 14 oxide perovskite-based candidates with low thermal conductivity, and stable high-temperature performance for use as next-generation thermal barrier coatings	21
Halide perovskite	Photovoltaics	DFT + experimental	VASP	Developed a dimensional engineering strategy to grow controlled 1D and 2D LDPs on 3D perovskites. Demonstrated improved charge transport and record stability under ISOS-L-3 testing. Achieved 24.19% PCE (cell) and 22.05% *PCE* (module) with excellent long-term stability	128
Chalcogenide perovskite	Photovoltaics	DFT + device simulation	Quantum ESPRESSO + SCAPS-1D	Predicted the photovoltaic potential of lead-free chalcogenide perovskite analogue Na_3SbSe_4 using DFT and SCAPS-1D simulation, revealing a direct band gap, strong visible-range absorption, and device-level efficiency up to 28%, guiding the design of eco-friendly solar materials	132

Table 3 (*continued*)

LFP type	Application studied	Method used	Computational tool used	Key concept	Ref.
Halide perovskite	Band gap prediction and high-throughput modeling	DFT + surrogate modeling	VASP + SPuDS + PySPuDS + pymatgen	Developed an orthorhombic surrogate model (OSM) that replicates polymorphous network band gaps of ABX_3 halide perovskites with <0.1 eV error, enabling 10× faster high-throughput DFT screening for optoelectronic applications	143
Vacancy-ordered double perovskite	Stability prediction and materials design	DFT + ML	VASP + Symbolic Regression (custom algorithm)	Developed a symbolic regression–based explicit stability descriptor for A_2BX_6 vacancy-ordered double perovskites, achieving ∼90% accuracy in predicting decomposition energies, and enabling rapid, interpretable screening of stable, lead-free candidates	137
Ruddlesden–Popper perovskite	Neuromorphic computing	DFTB + experimental	Amsterdam modeling suite 2021	Engineered microstructure in lead-free 2D perovskite (PEA_2SnI_4) memristors to modulate Ag filament dynamics, enabling tuneable resistive switching, and synaptic behavior for neuromorphic applications through combined experimental–theoretical analysis	20
Vacancy-ordered double perovskite	Optoelectronics and gas sensing	DFT + experimental	Not specified	Developed mid-IR emitting $Cs_2AgIn_{1-x}TmxCl_6$-ZBLAY perovskite glass with 3.46 μm emission matched to HCl absorption for gas sensing; demonstrated excellent thermal and photostability	145
Hybrid organic–inorganic perovskite	Optoelectronics	DFT + experimental	VASP	Developed an organic–inorganic hybrid strategy using MA^+ and FA^+ to induce lattice distortion, enhancing the PLQY of non-doped DPNCs up to 15.4% by brightening the self-trapped exciton state	146
Double perovskite	Optoelectronics, thermoelectrics	DFT + Boltzmann transport theory	WIEN2k + BoltzTraP	Investigated electronic, optical, and thermoelectric properties of A_2AuSbZ_6 compounds; demonstrated structural stability, high *ZT* values, and visible-light transparency, highlighting their potential for green energy applications	135
Halide perovskite	Photovoltaics	ML + DFT + device simulation	CASTEP+ SCAPS-1D + Ridge	Combined DFT and SCAPS-1D simulations with Ridge regression ML to model and optimized Ca_3AsI_3 solar cell performance; predicted 25.16% PCE, and identified defect density as critical	147
Vacancy-ordered double perovskite	Thermoelectrics	DFT + Boltzmann transport theory	WIEN2k + BoltzTraP	Explored structural, optoelectronic, and thermoelectric properties using DFT and BTE-based BoltzTraP; identified low κ, high *ZT*, and visible-range bandgaps	19
Halide perovskite	Photovoltaics	DFT	QuantumATK	Systematic benchmarking of XC functionals, and DFT parameters (PPs, *k*-points, DMC) to optimize bandgap predictions with MGGA, showing low deviation at reduced cost	148
Double perovskite	Optoelectronics, thermoelectrics	DFT + Boltzmann transport theory	WIEN2k + BoltzTraP	First-principles study revealed Sr_2YBiO_6 as an indirect bandgap semiconductor (2.15 eV) with promising optical absorption, and thermoelectric performance (*ZT* up to 0.7 at 1200 K)	136
Halide perovskite	Photovoltaics	Device simulation + ML	SCAPS-1D + Python ML libraries	Developed and validated a machine learning model (RF) trained on 101 250 simulated solar cell configurations to predict and optimize PCE in compositionally engineered halide-based tin perovskites; top PCEs ranged from 5.34% to 11.69%	129
Halide perovskite	Photovoltaics	ML	CatBoost, SHAP, Optuna	Developed ML models to predict bandgap, VBM, and CBM for 551 absorber compositions; CatBoost achieved RMSE of 0.054eV for bandgap; validated on 13 unseen compounds, and analyzed feature impact using SHAP	149
Halide perovskite	Optoelectronics	DFT + experimental	VASP	Benign mid-gap halide vacancy states in 2D-bismuth-based halide perovskite microcrystals for enhanced broadband photodetectors	150
Hybrid organic–inorganic perovskite	Photovoltaics	DFT + ML	Gaussian16 + gplearn (GP-SR), SISSO, SHAP	An interpretable ML model discovers two universal descriptors (Φ_1, Φ_2) for accurate PCE prediction. Φ_2 outperforms E_g in predictive power; high-throughput screening enabled	133

Table 3 (*continued*)

LFP type	Application studied	Method used	Computational tool used	Key concept	Ref.
Halide perovskite	Thermoelectrics, spintronics, optoelectronics	DFT + Boltzmann transport theory	WIEN2k + BoltzTraP	Doping $CsZnBr_3$ with C or N induces ferromagnetism and spin-filter behavior, enhancing thermoelectric (*ZT* up to 1.06 at 1200 K) and UV-range optoelectronic performance	99
Oxide perovskite	Gas sensing	ML	Word2Vec + CGCNN + Transfer Learning	Developed a deep learning framework combining NLP and CGCNN to predict high-performing gas-sensing TMPOs; validated with selective 3H-2B detection (LOD: 25 ppb)	142
Oxide perovskite	Thermoelectrics, photovoltaics	DFT + Boltzmann transport theory	DFT + BoltzTraP	Ni substitution narrows the bandgap, enhances optical absorption, and *ZT* (0.90–0.99)	140
Oxide perovskite	Photovoltaics	DFT + device simulation	Quantum ESPRESSO + OghmaNano	Developed a combined DFT and OghmaNano device modeling approach to evaluate lead-free Sm_2NiMnO_6 for PSCs, achieving tuneable bandgaps, high photoconductivities, and up to 9% theoretical PCEs	131
Double perovskite	Photovoltaics	Device simulation + ML	SCAPS-1D + Python (ML)	Combined SCAPS-1D simulation and ML prediction to optimize $Cs_2AgBiBr6$-based PSCs with GQD HTL, achieving 15.33% *PCE* and 96.03% ML prediction accuracy	120
Double perovskite	Photovoltaics	Device simulation	SCAPS-1D	Simulated ITO/C60/Rb_2AlAgI_6/CBTS PSC achieving a PCE of 29.41%; investigated effects of thickness, temperature, defects, and resistances on performance	122
Halide perovskite	Photovoltaics	DFT	WIEN2k	Identified $CsEuBr_3$ as a stable, ductile, high-absorption material with a 1.2 eV bandgap and low loss function, confirming its suitability for photovoltaic applications	121
Halide perovskite	Photovoltaics	Device simulation	SCAPS-1D	Simulated three hybrid PSCs with IGZO ETL, and different HTLs (Cu_2O, CuO, SnSe). Device I (IGZO/Cu_2O) achieved 33.84% PCE, 1.13 V V_{oc}, 34.54 mA cm^{-2} J_{sc}, and 86.78% FF. Optimization of defects, thickness, recombination, and resistance showed strong potential for eco-friendly solar cells	127
Halide perovskite	Photovoltaics	Device simulation	SCAPS-1D	Optimized Cs_2TiBr_6-based solar cells with ZnSe ETL and V_2O_5 HTL and achieved a PCE of 31.02%. Simulation revealed the critical influence of absorber/transport layer thickness, defect density, and temperature. Device I (Al/FTO/ZnSe/Cs_2TiBr_6/V_2O_5/Os) outperformed others in terms of efficiency and FF	123
Double perovskite	Photovoltaics	Device simulation	SCAPS-1D	Optimized Rb_2LiGaI_6-based PSC using WS_2 as the ETL, and CuI as the HTL. Achieved a PCE of 28.71% with V_{oc} = 0.856 V, J_{sc} = 41.24 mA cm^{-2}, and FF = 81.24%. Performance boost attributed to high lattice stability and tuneable band structure of Rb_2LiGaI_6	130
Double perovskite	Photovoltaics	DFT	CASTEP	Assessed structural, electronic, optical, and mechanical properties of $K_2CuSbBr_6$. Found an indirect bandgap of 0.32 eV, strong absorption in the visible-NIR range, good ductility, and anisotropy	151
Oxide perovskite	Spintronics	DFT+*U*	Quantum ESPRESSO	Investigated a (010)-oriented $CaNbO_3$/Ca_2VMoO_6 heterostructure; found spin reorientation at the interface leading to antiferromagnetic coupling, and metallic behavior due to Mo t_2g states	141
Double perovskite	Photovoltaics	DFT + Boltzmann transport theory	Quantum ESPRESSO + BoltzTraP	Cation mixing (K/Cs) in Rb_2SnBr_6 tunes bandgap and mechanical flexibility, enhances thermoelectric performance (*ZT* up to 0.77), and enables application in optoelectronics and solar cells	152
Double perovskite	Photocatalysis	DFT + AIMD + ML	VASP, XGBoost, SISSO, ThermoPW	Developed a multistep ML framework and GW descriptor to predict quasiparticle band gaps with >90% accuracy; screened 94 lead-free candidates	138

Table 3 (*continued*)

LFP type	Application studied	Method used	Computational tool used	Key concept	Ref.
Double perovskite	Photovoltaic, Thermoelectric	DFT + Boltzmann transport theory	WIEN2k + BoltzTraP	Bandgap tuned from 1.5 to 0.9 eV *via* halide substitution; K_2InBiI_6 shows enhanced thermoelectric performance; strong visible-range absorption supports solar cell use	24
Double perovskite	Thermoelectrics, optoelectronics	DFT + Boltzmann transport theory	WIEN2k + BoltzTraP	Employed advanced DFT workflows to predict stable wide-bandgap fluoroperovskites ($Eg \approx 2.98$ eV) with strong UV-visible absorption, and high thermoelectric ZT (~ 0.99) at 300 K	124
Double perovskite	Photovoltaics	DFT + Boltzmann transport theory	WIEN2k + BoltzTraP	Predicted stable halide double perovskites with high PF, and ZT (~ 1), strong UV-visible absorption, and ductile nature, highlighting Ga_2PtI_6 as a dual-function material for optoelectronic, and thermoelectric applications	125
Double perovskite	Optoelectronics, spintronics	DFT	WIEN2k	Investigated Sr_2XWO_6 (X = Co, Zn); revealed spin-dependent bandgaps and half-metallicity in Sr_2CoWO_6, and strong UV-visible absorption, identifying it as a promising material for optoelectronic and spintronic applications	126
Double perovskite	Optoelectronics, thermoelectrics, photovoltaics	DFT	WIEN2k	Assessed lead-free K_2AuSbX_6 (X = Cl, Br, I) as stable cubic perovskites with tuneable band gaps, and optical response; K_2AuSbI_6 suited for visible-range photovoltaics, $K_2AuSbBr_6$ for thermoelectrics due to high Seebeck coefficient, and power factor	153
Oxide perovskite	Optoelectronics, spintronics	DFT + Birch–Murnaghan EOS, elastic tensor (IRelast)	WIEN2k + IRelast	Identified $BeSiO_3$ as a non-magnetic wide-gap semiconductor ($E_g \approx 2.64$–2.71 eV), and $PdSiO_3$ as a spin-polarized half-metal with strong UV sensitivity, supporting spintronic and UV-optoelectronic applications	154
Oxide perovskite	Ferroelectric/ piezoelectric	DFT, DFPT	CASTEP	Sn displacement drives spontaneous polarization, making $SnTiO_3$ a stable lead-free ferroelectric candidate	116
Double perovskite	spintronics	DFT (GGA + U with SOC)	WIEN2K	Strong O_s–O hybridization suppresses the magnetic moment and stabilizes high-T antiferromagnetism	90
Halide perovskite	Photovoltaic, optoelectronics	ML + DFT	VASP	Over 480 halide LFPs screened; 10 new stable compounds found with visible-range bandgaps for optoelectronic use	119
Double perovskite	Photovoltaics	ML	GPR-NN, XGBoost, LGBM	GPR-NN predicts bandgap and formation energy with higher accuracy and feature interpretability	155
Halide perovskite	Photovoltaics	DFT + device simulation	WIEN2K, SCAPS-1D	$RbSnBr_3$ and $RbSnCl_3$ show ideal bandgaps and high simulated PCEs as Pb-free absorber layers	103
Hybrid organic–inorganic perovskite	Photovoltaics	DFT (HSE06, PBE) + MD + optical simulation	VASP, PWmat, COMSOL	A-, B-, and X-site mixing yields stable Pb-free HOIPs with direct bandgaps and $>90\%$ absorption across 300–1200 nm	134

throughput simulation and descriptor-based machine learning models,[100,133] as explained in Table 3 and Section 5.

Computational lead-free perovskite research is maturing into a highly targeted, application-focused field, driven by methodological convergence, machine learning integration, and cross-functional material versatility. Trends such as stability modeling, defect tolerance assessment, and advanced design strategies are ensuring that performance gains are paired with durability, while scalable, high-throughput workflows are accelerating the path from theoretical prediction to real-world deployment across different application areas.

7. Challenges and future outlook

As computational studies of LFPs have matured, several challenges and opportunities for future progress have become clear. Underrepresented material families such as chalcogenide, oxynitride, and Cu-based perovskites are rarely modeled despite strong potential *e.g.*, Na_3SbSe_4.[132] Dynamic effects including ion migration, phonon scattering, and interface degradation are also insufficiently addressed in most current frameworks (Section 5). In addition, experimental validation of computational predictions remains limited, underscoring the need for tighter integration between theory and synthesis.

To close these gaps, and guide the next phase of research, several priorities are clear:

- Broaden chemical screening to include less-explored LFP chemistries with promising optoelectronic, and thermoelectric behavior.
- Adopt multiscale simulation approaches that connect electronic, atomistic, and device-level processes.
- Develop explainable and physically grounded ML models to support generalization across material classes.
- And strengthen computational–experimental feedback loops for iterative design and validation.

Taken together, the trends captured in Table 3 and analysed in Sections 4 and 5 reflect a field converging toward modular, interpretable, and application-aware computational materials design. As methods and models continue to evolve, the path forward lies in expanding compositional diversity, incorporating greater physical realism, and translating computational advances into experimental impact, ultimately driving sustainable, high-performance lead-free perovskite technologies.

8. Conclusion

This review has mapped the computational landscape of lead-free perovskite research across more than a decade (2013–2025) of methodological evolution and application diversification. Through bibliometric and thematic analyses, we have shown that computational studies have not only accelerated the discovery of promising LFP materials but have also reshaped the structure of inquiry from elemental screening to device-level optimization. Beginning with density functional theory as a foundational tool, the field has embraced a broader ecosystem of methods including hybrid functionals, *ab initio* molecular dynamics, machine learning, and device simulation frameworks.

These advancements have enabled a shift from isolated property prediction to integrating multiscale modeling approaches. Simultaneously, the application space has expanded beyond photovoltaics into areas such as spintronics, neuromorphic computing, photocatalysis, and thermoelectrics, each supported by tailored computational strategies. Our analysis highlights that this progress is rooted in the intrinsic versatility of LFP materials and the growing sophistication of computational workflows. The tight coupling between material class, targeted properties, and chosen computational tools reflects a maturing discipline capable of addressing complex technological requirements with increasing precision.

As the field moves forward, the convergence of data-centric modeling, high-throughput computation, and application-specific simulation is expected to accelerate LFP innovation further. The following steps should continue to advance the development of explainable machine learning models and modular simulation frameworks that unify electronic, structural, and device-level modeling. While promising efforts are already emerging in this space, further studies are needed to standardize these approaches, broaden their applicability across LFP chemistries, and validate them against experimental benchmarks. Such efforts will be essential to enhance interpretability, reproducibility, and the real-world translation of computational insights. By serving as a comprehensive synthesis of these developments, this review aims to provide both a reference point and a roadmap for future work in computational materials design for sustainable, lead-free technologies.

Consent to participate

Informed consent was obtained from all authors.

Consent to publish

All authors provided consent for the publication of this work.

Ethical approval

Not applicable.

Author contributions

S. K. F. was responsible for data curation, analysis of the review table, drafting, and structuring the manuscript, and developing comparative insights across material systems and computational methods. K. Z., R. H. A., and M. A. were responsible for conceptualization, comparative analysis, and supervision. S. K. F., R. A., and M. H. A. were responsible for drafting the manuscript and literature analysis. All authors were actively part of the writing, revision, and discussion.

Conflicts of interest

The authors declare no competing interests.

Data availability

This review is based on data extracted and analysed from published research articles, with all sources fully cited in the reference list. No new data were generated or analysed in this study.

Acknowledgements

This project was funded by the Research Office at the United Arab Emirates University (UAEU), Strategic Research Program (funded by the National Water and Energy Center, G00005000). The authors acknowledge the Department of Chemistry, and the College of Science at the United Arab Emirates University (UAEU), Al Ain, UAE.

References

1 S. Wu, Z. Chen, H. L. Yip and A. K. Jen, The evolution and future of metal halide perovskite-based optoelectronic devices, *Matter*, 2021, **4**(12), 3814–3834.
2 H. Dong, C. Ran, W. Gao, M. Li, Y. Xia and W. Huang, Metal Halide Perovskite for next-generation optoelectronics: progresses and prospects, *ELight*, 2023, **3**(1), 3.
3 X. Wang, T. Li, B. Xing, M. Faizan, K. Biswas and L. Zhang, Metal halide semiconductors beyond lead-based perovskites for promising optoelectronic applications, *J. Phys. Chem. Lett.*, 2021, **12**(43), 10532–10550.
4 Y. Gao, Y. Pan, F. Zhou, G. Niu and C. Yan, Lead-free halide perovskites: a review of the structure–property relationship and applications in light emitting devices and radiation detectors, *J. Mater. Chem. A*, 2021, **9**(20), 11931–11943.
5 Y. Zhang, Y. Ma, Y. Wang, X. Zhang, C. Zuo, L. Shen and L. Ding, Lead-free perovskite photodetectors: progress, challenges, and opportunities, *Adv. Mater.*, 2021, **33**(26), 2006691.
6 C. C. Li, T. Y. Huang, Y. H. Lai, Y. C. Huang and C. S. Tan, Lead-free perovskites for flexible optoelectronics, *Mater. Today Electron.*, 2024, **8**, 100095.
7 I. López-Fernández, D. Valli, C. Y. Wang, S. Samanta, T. Okamoto, Y. T. Huang, K. Sun, Y. Liu, V. S. Chirvony, A. Patra and J. Zito, Lead-free halide perovskite materials and optoelectronic devices: progress and prospective, *Adv. Funct. Mater.*, 2024, **34**(6), 2307896.
8 P. K. Nayak, S. Mahesh, H. J. Snaith and D. Cahen, Photovoltaic solar cell technologies: analysing the state of the art, *Nat. Rev. Mater.*, 2019, **4**(4), 269–285.
9 A. Rogalski, F. Wang, J. Wang, P. Martyniuk and W. Hu, The perovskite optoelectronic devices–A look at the future, *Small Methods*, 2025, **9**(1), 2400709.
10 M. Abdellah, S. Zhang, M. Wang and L. Hammarstrom, Competitive hole transfer from CdSe quantum dots to thiol ligands in CdSe-cobaloxime sensitized NiO films used as photocathodes for H2 evolution, *ACS Energy Lett.*, 2017, **2**(11), 2576–2580.
11 K. Žídek, K. Zheng, P. Chabera, M. Abdellah and T. Pullerits, Quantum dot photodegradation due to CdSe-ZnO charge transfer: Transient absorption study, *Appl. Phys. Lett.*, 2012, **100**(24), 243111.
12 A. H. Slavney, T. Hu, A. M. Lindenberg and H. I. Karunadasa, A bismuth-halide double perovskite with long carrier recombination lifetime for photovoltaic applications, *J. Am. Chem. Soc.*, 2016, **138**(7), 2138–2141; F. Brivio, A. B. Walker and A. Walsh, Structural and electronic properties of hybrid perovskites for high-efficiency thin-film photovoltaics from first-principles, *Appl. Mater.*, 2013, **1**(4), 042111; M. R. Filip, G. E. Eperon, H. J. Snaith and F. Giustino, Steric engineering of metal-halide perovskites with tunable optical band gaps, *Nat. Commun.*, 2014, **5**(1), 5757.
13 D. Meggiolaro and F. De Angelis, First-principles modeling of defects in lead halide perovskites: best practices and open issues, *ACS Energy Lett.*, 2018, **3**(9), 2206–2222.
14 K. T. Butler, D. W. Davies, H. Cartwright, O. Isayev and A. Walsh, Machine learning for molecular and materials science, *Nature*, 2018, **559**(7715), 547–555.
15 K. M. Jablonka, D. Ongari, S. M. Moosavi and B. Smit, Using collective knowledge to assign oxidation states of metal cations in metal–organic frameworks, *Nat. Chem.*, 2021, **13**(8), 771–777.
16 S. Curtarolo, W. Setyawan, S. Wang, J. Xue, K. Yang, R. H. Taylor, L. J. Nelson, G. L. Hart, S. Sanvito, M. Buongiorno-Nardelli and N. Mingo, AFLOWLIB. ORG: A distributed materials properties repository from high-throughput ab initio calculations, *Comput. Mater. Sci.*, 2012, **58**, 227–235.
17 J. Schmidt, M. R. Marques, S. Botti and M. A. Marques, Recent advances and applications of machine learning in solid-state materials science, *npj Comput. Mater.*, 2019, **5**(1), 83.
18 L. Zhang, G. X. Chen, Z. L. Wang, X. N. Liang, Q. Zhang and S. Liu, Automated machine learning guides discovery of ABO3-type oxides for effective water splitting photocatalysis, *Chem. Phys. Lett.*, 2025, **869**, 142034.
19 A. M. Tighezza, A. Nazir, E. A. Khera, M. Manzoor, M. Ishfaq and R. A. Sharma, DFT approach to study the vacancy ordered lead free double inorganic perovskites Na2PtX6 (X= Cl, Br) for sustainable technologies, *J. Inorg. Organomet. Polym. Mater.*, 2025, **35**(2), 1201–1218.
20 F. C. Wu, Z. M. Su, Y. C. Hsu, W. Y. Chou, W. C. Lai, C. C. Tsai and H. L. Cheng, Microstructure-modulated conductive filaments in Ruddlesden-Popper perovskite-based memristors and their application in artificial synapses, *Mater. Today Phys.*, 2025, **53**, 101708.
21 M. Zeraati, A. R. Oganov, A. P. Maltsev and S. F. Solodovnikov, Computational screening of complex oxides for next-generation thermal barrier coatings, *J. Appl. Phys.*, 2025, **137**(6), 065106.

22 H. Wei and J. Huang, Halide lead perovskites for ionizing radiation detection, *Nat. Commun.*, 2019, **10**(1), 1066.
23 A. Zaghrane, H. Ouhenou, E. Darkaoui, M. Agouri, A. Abbassi, Y. Mekaoui, S. Taj and B. Manaut, First-principles investigation of structural, electronic, optical, and magnetic properties of a scintillating double perovskite halides (Cs_2LiCeX_6) with (X = F, Br, and I), *Chin. J. Phys.*, 2024, **90**, 911–921.
24 S. Nazir, N. A. Noor, F. Majeed, S. Mumtaz and K. M. Elhindi, First-Principles Calculations of Halide Double Perovskite K2InBiX6 (X = Cl, Br, I) for Solar Cell Applications, *J. Inorg. Organomet. Polym. Mater.*, 2025, 1–5.
25 M. A. Rehman, Z. U. Rehman, M. Usman, A. A. Ifseisi, J. Fatima, M. E. Assal and A. Hamad, The photocatalytic degradation performance of Dion-Jacobson-type layered perovskites AMCa2Ta3O10 (AM= Rb, Cs): A DFT study, *J. Solid State Chem.*, 2024, **337**, 124809.
26 B. W. Zhang, J. A. Steele, A. Baktash, S. Zhang, F. Chen, C. H. Lin, E. Solano, A. E. Rezaee, S. Gaznaghi, E. Q. Han and Y. Zhang, Manipulation of ionic transport in anisotropic silver-based lead-free perovskite analogue with interstitial-iodide for enabling artificial synaptic functions, *Nano Energy*, 2025, **139**, 110981.
27 M. R. Filip and F. Giustino, The geometric blueprint of perovskites, *Proc. Natl. Acad. Sci. U. S. A.*, 2018, **115**(21), 5397–5402.
28 B. Saparov and D. B. Mitzi, Organic–inorganic perovskites: structural versatility for functional materials design, *Chem. Rev.*, 2016, **116**(7), 4558–4596.
29 R. H. Alzard, L. A. Siddig, A. S. Abdelhamid, T. Ramachandran and A. Alzamly, Structural analysis and photocatalytic activities of bismuth-lanthanide oxide perovskites, *J. Solid State Chem.*, 2024, **329**, 124359.
30 G. Volonakis, M. R. Filip, A. A. Haghighirad, N. Sakai, B. Wenger, H. J. Snaith and F. Giustino, Lead-free halide double perovskites *via* heterovalent substitution of noble metals, *J. Phys. Chem. Lett.*, 2016, **7**(7), 1254–1259.
31 E. Greul, M. L. Petrus, A. Binek, P. Docampo and T. Bein, Highly stable, phase pure Cs 2 AgBiBr 6 double perovskite thin films for optoelectronic applications, *J. Mater. Chem. A*, 2017, **5**(37), 19972–19981.
32 L. N. Quan, M. Yuan, R. Comin, O. Voznyy, E. M. Beauregard, S. Hoogland, A. Buin, A. R. Kirmani, K. Zhao, A. Amassian and D. H. Kim, Ligand-stabilized reduced-dimensionality perovskites, *J. Am. Chem. Soc.*, 2016, **138**(8), 2649–2655.
33 A. M. Ganose, J. Park, A. Faghaninia, R. Woods-Robinson, K. A. Persson and A. Jain, Efficient calculation of carrier scattering rates from first principles, *Nat. Commun.*, 2021, **12**(1), 2222.
34 P. Kayastha, E. Fransson, P. Erhart and L. Whalley, Octahedral tilt-driven phase transitions in BaZrS3 chalcogenide perovskite, *J. Phys. Chem. Lett.*, 2025, **16**(8), 2064–2071.
35 H. Jin, E. Debroye, M. Keshavarz, I. G. Scheblykin, M. B. Roeffaers, J. Hofkens and J. A. Steele, It's a trap! On the nature of localised states and charge trapping in lead halide perovskites, *Mater. Horiz.*, 2020, **7**(2), 397–410.
36 P. Honarmandi and R. Arróyave, Uncertainty quantification and propagation in computational materials science and simulation-assisted materials design, *Integr. Mater. Manuf. Innov.*, 2020, **9**(1), 103–143.
37 B. Sanchez-Lengeling and A. Aspuru-Guzik, Inverse molecular design using machine learning: Generative models for matter engineering, *Science*, 2018, **361**(6400), 360–365.
38 C. J. Bartel, C. Sutton, B. R. Goldsmith, R. Ouyang, C. B. Musgrave, L. M. Ghiringhelli and M. Scheffler, New tolerance factor to predict the stability of perovskite oxides and halides, *Sci. Adv.*, 2019, **5**(2), eaav0693.
39 W. Zhang, G. E. Eperon and H. J. Snaith, Metal halide perovskites for energy applications, *Nat. Energy*, 2016, **1**(6), 1–8.
40 C. Quarti, E. Mosconi and F. De Angelis, Interplay of orientational order and electronic structure in methylammonium lead iodide: implications for solar cell operation, *Chem. Mater.*, 2014, **26**(22), 6557–6569.
41 A. Jain, S. P. Ong, G. Hautier, W. Chen, W. D. Richards, S. Dacek, S. Cholia, D. Gunter, D. Skinner, G. Ceder and K. A. Persson, Commentary: The Materials Project: A materials genome approach to accelerating materials innovation, *APL Mater.*, 2013, **1**(1), 011002.
42 F. Jamalinabijan, S. Alidoust, G. I. Demir and A. Tekin, Discovering novel lead-free mixed cation hybrid halide perovskites *via* machine learning, *Phys. Chem. Chem. Phys.*, 2025, **27**(14), 7389–7398.
43 C. Zhu, Y. Liu, D. Wang, Z. Zhu, P. Zhou, Y. Tu, G. Yang, H. Chen, Y. Zang, J. Du and W. Yan, Exploration of highly stable and highly efficient new lead-free halide perovskite solar cells by machine learning, *Cell Rep. Phys. Sci.*, 2024, **5**(12), 102321.
44 M. R. Filip, S. Hillman, A. A. Haghighirad, H. J. Snaith and F. Giustino, Band gaps of the lead-free halide double perovskites Cs2BiAgCl6 and Cs2BiAgBr6 from theory and experiment, *J. Phys. Chem. Lett.*, 2016, **7**(13), 2579–2585.
45 P. Bhatt, A. K. Pandey, A. Rajput, K. K. Sharma, A. Moyez and A. Tewari, A review on computational modeling of instability and degradation issues of halide perovskite photovoltaic materials, *Wiley Interdiscip. Rev.: Comput. Mol. Sci.*, 2023, **13**(6), e1677.
46 G. A. Nowsherwan, S. Riaz and S. Naseem, Predictive modeling of CsFABiCuI6-based PSC with Nd-doped ZnO as ETL using machine learning and numerical simulation, *Multiscale Multidiscip. Model. Exp. Des.*, 2025, **8**(6), 1–23.
47 F. Tayari, S. S. Teixeira, M. P. Graca and K. I. Nassar, Progress and developments in the fabrication and characterization of metal halide perovskites for photovoltaic applications, *Nanomaterials*, 2025, **15**(8), 613.
48 A. Shukla, V. K. Sharma, S. K. Gupta and A. S. Verma, Computational determination of the physical-thermoelectric parameters of tin-based organomatallic halide perovskites (CH3NH3SnX3, X= Br and I): Emerging materials for optoelectronic devices, *Mater. Chem. Phys.*, 2020, **253**, 123389.
49 T. Lu, H. Li, M. Li, S. Wang and W. Lu, Inverse design of hybrid organic–inorganic perovskites with suitable

bandgaps *via* proactive searching progress, *ACS Omega*, 2022, **7**(25), 21583–21594.

50 A. Mansouri Tehrani, A. O. Oliynyk, M. Parry, Z. Rizvi, S. Couper, F. Lin, L. Miyagi, T. D. Sparks and J. Brgoch, Machine learning directed search for ultraincompressible, superhard materials, *J. Am. Chem. Soc.*, 2018, **140**(31), 9844–9853.

51 J. Noh, J. Kim, H. S. Stein, B. Sanchez-Lengeling, J. M. Gregoire, A. Aspuru-Guzik and Y. Jung, Inverse design of solid-state materials *via* a continuous representation, *Matter*, 2019, **1**(5), 1370–1384.

52 T. Tsuchiya and J. Tsuchiya, High-pressure–high-temperature phase relations of MgGeO3: First-principles calculations, *Phys. Rev. B:Condens. Matter Mater. Phys.*, 2007, **76**(9), 092105.

53 C. C. Stoumpos, C. D. Malliakas and M. G. Kanatzidis, Semiconducting tin and lead iodide perovskites with organic cations: phase transitions, high mobilities, and near-infrared photoluminescent properties, *Inorg. Chem.*, 2013, **52**(15), 9019–9038.

54 E. T. McClure, M. R. Ball, W. Windl and P. M. Woodward, Cs2AgBiX6 (X= Br, Cl): new visible light absorbing, lead-free halide perovskite semiconductors, *Chem. Mater.*, 2016, **28**(5), 1348–1354.

55 H. C. Herbol, W. Hu, P. Frazier, P. Clancy and M. Poloczek, Efficient search of compositional space for hybrid organic–inorganic perovskites *via* Bayesian optimization, *npj Comput. Mater.*, 2018, **4**(1), 51.

56 J. Im, S. Lee, T. W. Ko, H. W. Kim, Y. Hyon and H. Chang, Identifying Pb-free perovskites for solar cells by machine learning, *npj Comput. Mater.*, 2019, **5**(1), 37.

57 G. X. Zhang, Y. Song, W. Zhao, H. An and J. Wang, Machine learning-facilitated multiscale imaging for energy materials, *Cell Rep. Phys. Sci.*, 2022, **3**(9), 101008.

58 S. Axelrod, D. Schwalbe-Koda, S. Mohapatra, J. Damewood, K. P. Greenman and R. Gómez-Bombarelli, Learning matter: Materials design with machine learning and atomistic simulations, *Acc. Mater. Res.*, 2022, **3**(3), 343–357.

59 U. Aeberhard, N. Natsch, A. Schneider, S. J. Zeder, H. Carrillo-Nuñez, B. Blülle and B. Ruhstaller, Multi-Scale Simulation of Reverse-Bias Breakdown in All-Perovskite Tandem Photovoltaic Modules under Partial Shading Conditions, *Solar RRL*, 2024, **8**(21), 2400492.

60 E. T. Chenebuah, M. Nganbe and A. B. Tchagang, A deep generative modeling architecture for designing lattice-constrained perovskite materials, *npj Comput. Mater.*, 2024, **10**(1), 198.

61 J. Moon, W. Beker, M. Siek, J. Kim, H. S. Lee, T. Hyeon and B. A. Grzybowski, Active learning guides discovery of a champion four-metal perovskite oxide for oxygen evolution electrocatalysis, *Nat. Mater.*, 2024, **23**(1), 108–115.

62 S. Sun, N. T. Hartono, Z. D. Ren, F. Oviedo, A. M. Buscemi, M. Layurova, D. X. Chen, T. Ogunfunmi, J. Thapa, S. Ramasamy and C. Settens, Accelerated development of perovskite-inspired materials *via* high-throughput synthesis and machine-learning diagnosis, *Joule*, 2019, **3**(6), 1437–1451.

63 J. Zhang, J. Wu, V. M. Le Corre, J. A. Hauch, Y. Zhao and C. J. Brabec, Advancing perovskite photovoltaic technology through machine learning-driven automation, *InfoMat*, 2025, **7**(5), e70005.

64 M. Omidvar, H. Zhang, A. A. Ihalage, T. G. Saunders, H. Giddens, M. Forrester, S. Haq and Y. Hao, Accelerated discovery of perovskite solid solutions through automated materials synthesis and characterization, *Nat. Commun.*, 2024, **15**(1), 6554.

65 A. Dubey, S. L. Sanchez, J. Yang and M. Ahmadi, Lead-free halide perovskites for photocatalysis *via* high-throughput exploration, *Chem. Mater.*, 2024, **36**(5), 2165–2176.

66 J. Kirman, A. Johnston, D. A. Kuntz, M. Askerka, Y. Gao, P. Todorović, D. Ma, G. G. Privé and E. H. Sargent, Machine-learning-accelerated perovskite crystallization, *Matter*, 2020, **2**(4), 938–947.

67 M. D. Jones, J. A. Dawson, S. Campbell, V. Barrioz, L. D. Whalley and Y. Qu, Modelling interfaces in thin-film photovoltaic devices, *Front. Chem.*, 2022, **10**, 920676.

68 X. Shi, G. Zhang, Y. Lu and H. Pang, Applications of machine learning in electrochemistry, *Renewables*, 2023, **1**(6), 668–693.

69 A. Jain, Y. Shin and K. A. Persson, Computational predictions of energy materials using density functional theory, *Nat. Rev. Mater.*, 2016, **1**(1), 1–3.

70 A. W. Harzing (2007) Publish or Perish, available from **https://harzing.com/resources/publish-or-perish** [Accessed 26 April 2025].

71 A. Martín-Martín, E. Orduna-Malea and M. Thelwall, Delgado-López-Cózar E. Google Scholar, Web of Science, and Scopus: Which is best for me? Impact of Social Sciences Blog. 2019.

72 M. J. Page, J. E. McKenzie, P. M. Bossuyt, I. Boutron, T. C. Hoffmann, C. D. Mulrow, L. Shamseer, J. M. Tetzlaff, E. A. Akl, S. E. Brennan and R. Chou The PRISMA 2020 statement: an updated guideline for reporting systematic reviews. bmj. 2021;372.

73 P. Lopez, GROBID: Combining automatic bibliographic data recognition and term extraction for scholarship publications, in *International conference on theory and practice of digital libraries*, 2009, Springe, Berlin Heidelberg, pp. 473–474.

74 Q. Tao, P. Xu, M. Li and W. Lu, Machine learning for perovskite materials design and discovery, *npj Comput. Mater.*, 2021, **7**(1), 23.

75 H. Uratani and K. Yamashita, Charge carrier trapping at surface defects of perovskite solar cell absorbers: a first-principles study, *J. Phys. Chem. Lett.*, 2017, **8**(4), 742–746.

76 Y. Zhao and K. Zhu, Organic–inorganic hybrid lead halide perovskites for optoelectronic and electronic applications, *Chem. Soc. Rev.*, 2016, **45**(3), 655–689.

77 K. A. Bush, A. F. Palmstrom, Z. J. Yu, M. Boccard, R. Cheacharoen, J. P. Mailoa, D. P. McMeekin, R. L. Hoye, C. D. Bailie, T. Leijtens and I. M. Peters, 23.6%-efficient monolithic perovskite/silicon tandem solar cells with improved stability, *Nat. Energy*, 2017, **2**(4), 1–7.

78 F. Fu, J. Li, T. C. Yang, H. Liang, A. Faes, Q. Jeangros, C. Ballif and Y. Hou, Monolithic perovskite-silicon tandem solar cells: from the lab to fab?, *Adv. Mater.*, 2022, **34**(24), 2106540.
79 H. Min, D. Y. Lee, J. Kim, G. Kim, K. S. Lee, J. Kim, M. J. Paik, Y. K. Kim, K. S. Kim, M. G. Kim and T. J. Shin, Perovskite solar cells with atomically coherent interlayers on SnO2 electrodes, *Nature*, 2021, **598**(7881), 444–450.
80 P. Hohenberg and W. Kohn, Inhomogeneous electron gas, *Phys. Rev.*, 1964, **136**(3B), B864.
81 W. Kohn and L. J. Sham, Self-consistent equations including exchange and correlation effects, *Phys. Rev.*, 1965, **140**(4A), A1133.
82 R. G. Parr, S. R. Gadre and L. J. Bartolotti, Local density functional theory of atoms and molecules, *Proc. Natl. Acad. Sci. U. S. A.*, 1979, **76**(6), 2522–2526.
83 N. Argaman and G. Makov, Density functional theory: An introduction, *Am. J. Phys.*, 2000, **68**(1), 69–79.
84 A. D. Becke, Density-functional thermochemistry. III. The role of exact exchange, *J. Chem. Phys.*, 1993, **98**(7), 5648–5652.
85 D. J. Singh Density functional theory and applications to transition metal oxides. Lecture Notes of the Autumn School Correlated Electrons. 2012:2-1.
86 L. Leppert, First Principles Atomistic Theory of Halide Perovskites, *Halide Perovskite Semiconductors: Structures, Characterization, Properties, and Phenomena*, 2024, 215–250.
87 P. Blaha, K. Schwarz, F. Tran, R. Laskowski, G. K. Madsen and L. D. Marks, WIEN2k: An APW+ lo program for calculating the properties of solids, *J. Chem. Phys.*, 2020, **152**(7), 074101.
88 G. Kresse and J. Furthmüller, Efficient iterative schemes for ab initio total-energy calculations using a plane-wave basis set, *Phys. Rev. B:Condens. Matter Mater. Phys.*, 1996, **54**(16), 11169.
89 S. Zhao, K. Yamamoto, S. Iikubo, S. Hayase and T. Ma, First-principles study of electronic and optical properties of lead-free double perovskites Cs2NaBX6 (B= Sb, Bi; X= Cl, Br, I), *J. Phys. Chem. Solids*, 2018, **117**, 117–121.
90 A. E. Taylor, R. Morrow, D. J. Singh, S. Calder, M. D. Lumsden, P. M. Woodward and A. D. Christianson, Magnetic order and electronic structure of the 5d3 double perovskite Sr2 ScOsO6, *Phys. Rev. B:Condens. Matter Mater. Phys.*, 2015, **91**(10), 100406.
91 A. J. Cohen, P. Mori-Sánchez and W. Yang, Insights into current limitations of density functional theory, *Science*, 2008, **321**(5890), 792–794.
92 B. Himmetoglu, A. Floris, S. De Gironcoli and M. Cococcioni, Hubbard-corrected DFT energy functionals: The LDA+U description of correlated systems, *Int. J. Quantum Chem.*, 2014, **114**(1), 14–49.
93 A. Jain, G. Hautier, S. P. Ong, C. J. Moore, C. C. Fischer, K. A. Persson and G. Ceder, Formation enthalpies by mixing GGA and GGA+ U calculations, *Phys. Rev. B:Condens. Matter Mater. Phys.*, 2011, **84**(4), 045115.
94 R. Car and M. Parrinello, Unified approach for molecular dynamics and density-functional theory, *Phys. Rev. Lett.*, 1985, **55**(22), 2471.
95 S. Kumari, P. K. Kamlesh, L. Kumari, S. Kumar, S. Kumari, R. Singh, R. Gupta, M. S. Chauhan, U. Rani and A. S. Verma, Progress in theoretical study of lead-free halide double perovskite Na2AgSbX6 (X= F, Cl, Br, and I) thermoelectric materials, *J. Mol. Model.*, 2023, **29**(6), 195.
96 T. Gupta, D. Ghoshal, A. Yoshimura, S. Basu, P. K. Chow, A. S. Lakhnot, J. Pandey, J. M. Warrender, H. Efstathiadis, A. Soni and E. Osei-Agyemang, An environmentally stable and lead-free chalcogenide perovskite, *Adv. Funct. Mater.*, 2020, **30**(23), 2001387.
97 C. Gayner and K. K. Kar, Recent advances in thermoelectric materials, *Prog. Mater. Sci.*, 2016, **83**, 330–382.
98 E. Haque and M. A. Hossain, Electronic, phonon transport and thermoelectric properties of Cs2InAgCl6 from first-principles study, *Comput. Condensed Matter*, 2019, **19**, e00374.
99 R. Sharma, V. Revathi and V. Srivastava, Thermoelectric and optoelectronic features of C-and N-doped CsZnBr3 halide perovskite for use in spin filter and energy efficient devices, *Opt. Laser Technol.*, 2025, **181**, 111833.
100 H. Zou, H. Zhao, M. Lu, J. Wang, Z. Deng and J. Wang, Predicting thermodynamic stability of inorganic compounds using ensemble machine learning based on electron configuration, *Nat. Commun.*, 2025, **16**(1), 203.
101 A. S. Mosabbir, M. S. Sadek, M. Mahmood, M. M. Hosain, S. Sepeai, P. Chelvanathan, S. M. Sultan, K. Sopian, M. A. Ibrahim and K. Sobayel, Optimizing lead-free $Cs_2AgBiBr_6$ double perovskite solar cells: insights from SCAPS and FDTD simulations, *Sustainable Energy Fuels*, 2024, **8**(18), 4311–4323.
102 M. Shoab, Z. Aslam, M. Zulfequar and F. Khan, Numerical interface optimization of lead-free perovskite solar cells (CH3NH3SnI3) for 30% photo-conversion efficiency using SCAPS-1D, *Next Mater.*, 2024, **4**, 100200.
103 B. K. Ravidas, M. K. Roy and D. P. Samajdar, Design Insights and Photovoltaic Performance Analysis of Non-Lead Inorganic RbSnX3 (X= I, Br, Cl) Perovskites through Coupled Density Functional Theory and SCAPS-1D Simulation Frameworks, *ACS Appl. Electron. Mater.*, 2024, **6**(7), 5126–5150.
104 Y. Xiao, K. Choudhuri, A. Thanetchaiyakup, W. X. Chan, X. Hu, M. Sadek, Y. H. Tam, R. G. Loh, S. N. Shaik Mohammed, K. J. Lim and J. Z. Ten, Machine-Learning-Assisted Discovery of Mechanosynthesized Lead-Free Metal Halide Perovskites for the Oxidative Photocatalytic Cleavage of Alkenes, *Adv. Sci.*, 2024, **11**(29), 2309714.
105 A. M. Quraishi, A. Amina, S. Khan, S. H. Alrefaee, I. Shernazarov, A. Almahri, A. Nurmuhammedov, V. Tirth, A. Algahtani, R. M. Mohammed and Q. Mohsen, Insight into Structural, Electronic, Elastic and Optical properties of Thallium based Perovskite TlXBr3 (X= Ti, Zr) *via* DFT Study for reflective coating, *J. Inorg. Organomet. Polym. Mater.*, 2025, **35**(4), 3099–3110.

106 Z. Zhang, S. Wang, C. Chen, M. Sun, Z. Wang, Y. Cai, Y. Tuo, Y. Du, Z. Han, X. Yun and X. Guan, Design of photovoltaic materials assisted by machine learning and the mechanical tunability under micro-strain, *J. Mater. Sci. Technol.*, 2025, **227**, 108–121.

107 M. F. Rahman, M. N. Toki, M. R. Islam, P. Barman, S. Chowdhury, M. Rasheduzzaman and M. Z. Hasan, A computational study of electronic, optical, and mechanical properties of novel Ba3SbI3 perovskite using DFT, *Opt. Quantum Electron.*, 2024, **56**(2), 206.

108 M. A. Rahman, W. Hasan, M. Z. Hasan, A. Irfan, S. C. Mouna, M. A. Sarker, M. Z. Rahaman and M. Rahman, Structural, mechanical, electronic, optical and thermodynamic features of lead free oxide perovskites $AMnO_3$ (A = Ca, Sr, Ba): DFT simulation based comparative study, *Phys. B*, 2023, **668**, 415215.

109 L. J. Diguna, L. Jonathan, M. H. Mahyuddin, F. Maddalena, I. Mulyani, D. Onggo, A. Bachiri, M. E. Witkowski, M. Makowski, D. Kowal and W. Drozdowski, BA_2XBr_4 (X = Pb, Cu, Sn): from lead to lead-free halide perovskite scintillators, *Mater. Adv.*, 2022, **3**(12), 5087–5095.

110 J. M. Vicent-Luna, S. Apergi and S. Tao, Efficient computation of structural and electronic properties of halide perovskites using density functional tight binding: GFN1-xTB method, *J. Chem. Inf. Model.*, 2021, **61**(9), 4415–4424.

111 M. S. Uddin, M. K. Hossain, M. B. Uddin, G. F. Toki, M. Ouladsmane, M. H. Rubel, D. I. Tishkevich, P. Sasikumar, R. Haldhar and R. Pandey, An in-depth investigation of the combined optoelectronic and photovoltaic properties of lead-free Cs2AgBiBr6 double perovskite solar cells using DFT and SCAPS-1D frameworks, *Adv. Electron. Mater.*, 2024, **10**(5), 2300751.

112 F. Ji, J. Klarbring, F. Wang, W. Ning, L. Wang, C. Yin, J. S. Figueroa, C. K. Christensen, M. Etter, T. Ederth and L. Sun, Lead-free halide double perovskite Cs2AgBiBr6 with decreased band gap, *Angew. Chem.*, 2020, **132**(35), 15303–15306.

113 S. Belbahi, S. Labidi, R. Masrour and A. Hakamy, First-principles insights into the structural, electronic, magnetic, thermodynamic and elastic properties of Sr2SnMnO6 double perovskite oxide, *Chem. Phys.*, 2025, **595**, 112730.

114 Z. Zhang, S. Liu, Q. Xiong and Y. Liu, Strategic Integration of Machine Learning in the Design of Excellent Hybrid Perovskite Solar Cells, *J. Phys. Chem. Lett.*, 2025, **16**(3), 738–746.

115 Q. Sun, H. Chen and W. J. Yin, Do chalcogenide double perovskites work as solar cell absorbers: a first-principles study, *Chem. Mater.*, 2018, **31**(1), 244–250.

116 H. Ye, R. Zhang, D. Wang, Y. Cui, J. Wei, C. Wang, Z. Xu, S. Qu and X. Wei, First-principles calculation of lead-free perovskite $SnTiO_3$, *Int. J. Modern Phys. B*, 2013, **27**(24), 1350144.

117 X. Cai, Y. Li, J. Liu, H. Zhang, J. Pan and Y. Zhan, Discovery of all-inorganic lead-free perovskites with high photovoltaic performance *via* ensemble machine learning, *Mater. Horiz.*, 2023, **10**(11), 5288–5297.

118 W. Hu and L. Zhang, High-throughput calculation and machine learning of two-dimensional halide perovskite materials: Formation energy and band gap. Mater. Today, *Commun.*, 2023, **35**, 105841.

119 A. Jain, O. Voznyy and E. H. Sargent, High-throughput screening of lead-free perovskite-like materials for optoelectronic applications, *J. Phys. Chem. C*, 2017, **121**(13), 7183–7187.

120 M. A. Saifee, M. Ali, F. F. Khan, A. K. Srivastava, J. Ali and M. S. Khan, Design and performance optimization of a lead-free Cs2AgBiBr6 perovskite solar cell with graphene quantum dot hole transport layer using SCAPS-1D and machine learning, *J. Opt.*, 2025, 1.

121 M. Riaz, S. M. Ali, N. Bano, S. D. Ali and J. Ullah, Investigating structural, optoelectronic, and mechanical properties of europium-based halide perovskite CsEuBr3 for photovoltaic applications: a DFT approach, *Chem. Pap.*, 2025, **79**(2), 809–816.

122 O. Saidani, A. Yousfi, S. Bhattarai, M. R. Islame and G. S. Sahoo, Simulation insights into high-efficiency Rb2AlAgI6 hybrid perovskite solar cells: performance metrics and optimization strategies, *J. Opt.*, 2025, 1.

123 M. S. Reza, A. Ghosh, M. S. Reza, M. Aktarujjaman, M. J. Talukder, S. O. Aljazzar, J. Y. Al-Humaidi and Y. E. Mukhrish, Enhancing the Performance of Cs2TiBr6 Lead-Free Perovskite Solar Cells: A Simulation Study on the Impact of Electron and Hole Transport Layers, *Langmuir*, 2025, **41**(10), 6987–7007.

124 A. Nazir, A. Saxena, E. A. Khera, M. Manzoor, R. Sharma, A. A. Ibrahim, M. A. El-Meligy and B. Abdullaeva, Lead-Free double halide perovskite compounds: unveiling the structural, optoelectronic, and transport properties of A2TlRhF6 (A = K, Rb) for robust and sustainable green energy applications, *J. Inorg. Organomet. Polym. Mater.*, 2025, 1–8.

125 A. Nazir, E. A. Khera, M. Manzoor, S. Sahid, R. Sharma, R. Khan, N. Kamolova and T. Saidani, Role of Anion Variation in Physical Properties of Novel Vacancy Ordered Ga_2PtX_6 (X = Br and I) for Solar Cell and Thermoelectric Applications, *J. Inorg. Organomet. Polym. Mater.*, 2025, 1–7.

126 A. Nazir, E. A. Khera, Z. Anjum, A. A. Ghfar, Y. A. Kumar and R. Sharma, Theoretical Engineering of Structural, Electronic, and optical characteristics of double Perovskite Sr_2XWO_6 (X = co, zn) for Optical devices, *J. Inorg. Organomet. Polym. Mater.*, 2025, **35**(1), 409–419.

127 M. S. Reza, A. Ghosh, H. A. Ibrahium, M. B. Islam, M. H. Apu, M. S. Reza, M. I. Rahim and M. M. Akter, Optimizing charge transport layers to enhance the performance of lead-free RbGeI3 perovskite solar cells: a comprehensive analysis of ETL and HTL engineering, *Langmuir*, 2025, **41**(11), 7865–7885.

128 Y. Yun, Q. Chang, J. Yan, Y. Tian, S. Jiang, W. Wei, S. Li, Y. Guo, J. Yin, J. Li and M. Chen, Dimensional engineering of interlayer for efficient large-area perovskite solar cells with high stability under ISOS-L-3 aging test, *Sci. Adv.*, 2025, **11**(3), eadp3112.

129 P. Subudhi, S. Sivapatham, R. Narasimhan, B. Kumar and D. Punetha, Enhancing photovoltaic performance in tin-based perovskite solar cells: A unified approach utilizing numerical simulation and machine learning techniques, *J. Power Sources*, 2025, **639**, 236639.

130 U. U. Rehman, K. U. Sahar, Q. Wang, M. F. Rahman, E. Hussain and C. M. Wang, Numerical modeling and performance analysis of rubidium-based double perovskite solar cells: A comprehensive study, *J. Phys. Chem. Solids*, 2025, 112797.

131 T. Sangavi, S. Vasanth, C. Viswanathan and N. Ponpandian, Exploring Sm2NiMnO6 as a lead-free absorber for perovskite solar cells: Insights from theoretical and experimental approaches, *Sol. Energy Mater. Sol. Cells*, 2025, **283**, 113456.

132 X. Yu and Q. Gao, Design of a novel antimony-based solar cell by DFT and SCAPS simulation, *J. Comput. Electron.*, 2025, **24**(2), 1.

133 Y. Shi, J. Wen, C. Wen, L. Jiang, B. Wu, Y. Qiu and B. Sa, Interpretable machine learning insights of power conversion efficiency for hybrid perovskites solar cells, *Sol. Energy*, 2025, **290**, 113373.

134 R. Ali, Z. G. Zhu, Q. B. Yan, Q. R. Zheng, G. Su, A. Laref, C. S. Saraj and C. Guo, Compositional engineering study of lead-free hybrid perovskites for solar cell applications, *ACS Appl. Mater. Interfaces*, 2020, **12**(44), 49636–49647.

135 A. Usman, A. Ayyaz, Q. Mahmood, N. Algethami, S. A. Mahmoud, I. Boukhris and A. K. Alqorashi, Investigation of structural, optoelectronic, and transport properties of A2AuSbZ6 (A= Na, K, and Z= F, Cl) double perovskites for energy conversion applications, *J. Korean Ceram. Soc.*, 2025, 1–3.

136 A. Dixit, A. Saxena, M. Manzoor, S. Sahid, R. Sharma, A. A. Ibrahim, M. A. El-Meligy, B. Abdullaeva and V. Srivastava, DFT-Based investigation of opto-electronic, mechanical, and thermoelectric properties of Sr2YBiO6 for green energy applications, *J. Inorg. Organomet. Polym. Mater.*, 2025, 1–20.

137 X. Yang, Y. Han, P. Xu and F. Liu, Thermodynamic stability descriptor of A2BX6-type perovskite materials, *Mater. Chem. Phys.*, 2025, **333**, 130324.

138 G. Niu, Y. Wu, X. Chen, Y. Zhang, S. Yuan and J. Wang, Efficient and Accurate Prediction of Double Perovskite Quasiparticle Band Gaps *via* Machine Learning and a Descriptor, *J. Phys. Chem. Lett.*, 2025, **16**(16), 4006–4013.

139 W. Zhao, H. Ma, Z. Wang, B. Grégoire, A. Lin, S. Dai, X. Lin, T. Liang, J. Chen, T. Zhang and Y. Ding, Understanding double perovskite BCNF as a CO2 splitting catalyst for industrial decarbonisation, *Adv. Compos. Hybrid Mater.*, 2025, **8**(1), 1–2.

140 S. Z. Shah, S. Niaz, A. M. Saeedi, R. H. Althomali, M. M. Alghamdi, A. A. El–Zahhar and S. U. Asif, Designing Ni substituted double perovskite oxides Ba2Zn1-xNixWO6 (x = 0.00, 0.25, 0.50, 0.75, and 1.00) to explore the enhanced optoelectronic and thermoelectric performance using DFT, *Inorg. Chem. Commun.*, 2025, **174**, 114119.

141 A. Priyambada and P. Parida, Correlation-driven interface magnetism and conductivity in CaNbO3/Ca2VMoO6 perovskite oxide heterostructure: An ab initio approach, *J. Phys. Chem. Solids*, 2025, **203**, 112731.

142 S. Shao, L. Yan, J. Li, Y. Zhang, J. Zhang, H. W. Kim and S. S. Kim, Harnessing Transfer Deep Learning Framework for the Investigation of Transition Metal Perovskite Oxides with Advanced pn Transformation Sensing Performance, *ACS Sens.*, 2025, **10**(3), 1930–1947.

143 S. Yew, R. J. Morelock and C. B. Musgrave, Orthorhombic Structures as Inorganic Halide Perovskite Models for High-Throughput DFT Investigations, *J. Phys. Chem. C*, 2025, **129**(8), 4010–4024.

144 Y. Zhan, X. Ren, S. Zhao and Z. Guo, Accelerating the discovery of direct bandgap perovskites for solar energy *via* machine learning, *Mater. Today Commun.*, 2025, **45**, 112354.

145 X. Wang, X. Zhang, Y. Zhang, G. Liu, B. Zhou, L. Kong, J. Xu and L. Li, 3.46 μm mid-infrared emission from lead-free double perovskite fluorine glass and multi-wavelength array gas real-time monitoring applications in hydrogen energy, *Ceram. Int.*, 2025, **51**(18), 25269–25280.

146 C. Wang, F. Jiao, L. Zhang, Y. Wu and C. Zhan, Luminescent Inorganic–Organic Hybrid Nondoped Double Perovskite Nanocrystals for Optoelectronics, *ACS Appl. Nano Mater.*, 2025, **8**(16), 8511–8520.

147 M. S. Uddin, S. A. Rahman, M. A. Rahman, S. Mia, M. M. Rahman and M. S. Refat, Achieving over 28% efficiency in inorganic halide perovskite Ca3AsI3: Optimization of electron transport layers *via* DFT, SCAPS-1D, and machine learning, *J. Phys. Chem. Solids*, 2025, **200**, 112622.

148 D. S. Thakur, R. K. Sharma, V. Garg and S. Yadav, DFT-based accurate and efficient bandgap prediction of CsSnI3-xBrx and parameter optimization for enhanced perovskite solar cell performance, *Phys. B*, 2025, **697**, 416693.

149 S. Subba and S. Chatterjee, Machine learning-driven determination of key absorber layer parameters in perovskite solar cells, *Mater. Today Commun.*, 2025, **42**, 111113.

150 K. Singh, M. Hossain, P. K. Nayak, S. Karmakar, A. Tripathi, P. Sarkar, P. Rudra, A. M. Ali, G. K. Grandhi, P. Vivo and S. Mondal, Benign mid-gap halide vacancy states in 2D-bismuth-based halide perovskite microcrystals for enhanced broadband photodetectors, *Mater. Horiz.*, 2025, **12**(11), 3865–3877.

151 M. F. Rahman, T. Al Galib, M. Amami and L. B. Farhat, Exploring the structural, optical, electronic, and mechanical characteristics of the novel inorganic lead-free double perovskite K2CuSbBr6 for advanced optoelectronic devices, *Polyhedron*, 2025, **274**, 117513.

152 R. K. Pingak, A. Harbi, F. Nitti, S. Bouhmaidi, D. Tambaru, A. Z. Johannes, N. U. Hauwali, A. Wahid, M. Moutaabbid and L. Setti, The incorporation of Cs and K into the crystal structure of Rb2SnBr6 double perovskite: A DFT perspective, *Mater. Sci. Semicond. Process.*, 2025, **186**, 109044.

153 S. Nawaz, Y. Chen, X. Yan, M. Idrees and B. Amin, Structural, Optoelectronics and Thermoelectric Properties of K2AuSbX6 (X= Cl, Br, I) Halide Double Perovskites; DFT Study, *Comput. Condensed Matter*, 2025, e01050.

154 R. Ahmad, W. Ullah, N. Rahman, H. Albalawi, M. Husain, M. Hussien, V. Tirth, K. M. Abualnaja, G. Alosaimi, E. Almutib and Y. M. Alawaideh, DFT Analysis of Si-Based Oxide Perovskite for Optoelectronic Applications, *Silicon*, 2025, 1–2.

155 M. Nukunudompanich, H. Yoon, L. Hyojae, K. Kameda, M. Ihara and S. Manzhos, Machine learning of properties of lead-free perovskites with a neural network with additive kernel regression-based neuron activation functions, *MRS Adv.*, 2024, **9**(11), 857–862.